

1 **Drivers and vertical CO<sub>2</sub> flux balances budgets in a Sahelian *Faidherbia albida* agro-silvo-**  
2 **pastoral parkland: Insights from continuous high-frequency soil chamber measurements**  
3 **and Eddy Covariance.**

4 Seydina Mohamad Ba <sup>a d</sup>, Olivier Roupsard <sup>b c d</sup>, Lydie Chapuis-Lardy <sup>c f</sup>, Frédéric Bouvery <sup>g</sup>,  
5 Yélognissè Agbohessou <sup>h i j k</sup>, Maxime Duthoit <sup>c e</sup>, Aleksander Wieckowski <sup>k h</sup>, Torbern Tagesson <sup>k h</sup>,  
6 Mohamed Habibou Assouma <sup>l m n</sup>, Espoir K. Gaglo <sup>a d</sup>, Claire Delon <sup>m j</sup>, Bienvenu Sambou <sup>a</sup>, Dominique  
7 Serça <sup>m j</sup>

8 <sup>a</sup> Faculté des Sciences et Techniques (FST), Institut des Sciences de l'Environnement (ISE), Université  
9 Cheikh Anta Diop (UCAD) de Dakar, 5005, Dakar-Fann, Sénégal

10 <sup>b</sup> CIRAD, UMR Eco&Sols, Dakar, Sénégal

11 <sup>c</sup> Eco&Sols, Univ Montpellier, CIRAD, INRAE, Institut Agro, IRD, Montpellier, France

12 <sup>d</sup> LMI IESOL, Centre IRD-ISRA de Bel Air, Route des hydrocarbures, 18524, Dakar, Sénégal

13 <sup>e</sup> CIRAD, UMR Eco&Sols, Université de Montpellier, Cirad, INRAE, IRD, Institut Agro Montpellier, 2 place  
14 Viala, Montpellier, France

15 <sup>f</sup> IRD, UMR Eco&Sols, Université de Montpellier, Cirad, INRAE, IRD, Institut Agro Montpellier, 2 place Viala,  
16 Montpellier, France

17 <sup>g</sup> INRAE, 147 rue de l'Université, 75338 Paris, France

18 <sup>h</sup> [AIDA, Univ Montpellier, CIRAD, Montpellier, France](#)

19 <sup>i</sup> [CIRAD, UPR AIDA, Harare, Zimbabwe](#)

20 <sup>j</sup> [Department of Plant Production Sciences and Technologies, University of Zimbabwe, Harare, Zimbabwe](#)

21 <sup>k h</sup> Department of Physical Geography and Ecosystem Science, Lund University, Sölvegatan 12, S-223 62  
22 Lund, Sweden

23 <sup>l</sup> [CIRAD, UMR SELMET, dP ASAP, Bobo-Dioulasso, Burkina Faso](#)

24 <sup>m</sup> [UMR SELMET, CIRAD, INRAE, Univ Montpellier, Institut SupAgro, Montpellier, France](#)

25 <sup>n</sup> [Centre International de Recherche-Développement sur l'Élevage en zone Subhumide \(CIRDES\), N°559, rue  
26 -5-31 Avenue du Gouverneur Louveau, Bobo-Dioulasso, Burkina Faso](#)

27 <sup>m j</sup> Laboratoire d'Aérodynamique, Université de Toulouse, CNRS, IRD, 14 Avenue Edouard Belin, 31400 Toulouse,  
28 France

29 **Corresponding authors:**

30 Seydina Mohamad Ba: [seydina.ba@ird.fr](mailto:seydina.ba@ird.fr)

31 Olivier Roupsard: [olivier.roupsard@cirad.fr](mailto:olivier.roupsard@cirad.fr)

32 **Highlights:**

- 33 • Long-term high frequency CO<sub>2</sub> flux measurements using automated static  
34 chambers in a Sahelian *F. albida* parkland.
- 35 • Empirical gap-filling and flux partitioning methods validated against Eddy  
36 Covariance GPP.
- 37 • Fluxes peaked during the rainy season ~~in~~ both at a distance from trees in full sun  
38 (FS) and under tree canopies (Sh), driven mainly by soil moisture and leaf area.
- 39 • *F. albida* trees enhance CO<sub>2</sub> fluxes under canopies ("fertile island" effect) and  
40 account for ~23% ~~~50%~~ of annual ecosystem GPP.

41 **ABSTRACT:**

42 Agroforestry systems — combining trees with crops and/or livestock — are increasingly  
43 promoted as sustainable and climate-resilient land-use strategies. Despite their widespread  
44 presence in the Sahel, experimental data on their potential as carbon sinks are scarce. This study  
45 presents a full-year, high-frequency dataset of CO<sub>2</sub> fluxes in a Sahelian agro-silvo-pastoral  
46 parkland dominated by *F. Faidherbia albida*, located in Senegal's groundnut basin. CO<sub>2</sub> fluxes were  
47 continuously measured using automated static chambers, allowing the quantification of soil and  
48 crop respiration (R<sub>ch</sub>), gross primary production (GPP<sub>ch</sub>), and net carbon exchange (FCO<sub>2</sub>ch)  
49 under both full sun and shaded (under tree canopies) environments.

50 Seasonal patterns of CO<sub>2</sub> fluxes were similar in both environments, with peaks during the rainy  
51 season. R<sub>ch</sub> and GPP<sub>ch</sub> were significantly higher under tree canopies, indicating a 'fertile island'  
52 effect. CO<sub>2</sub> flux variability was primarily driven by soil moisture and leaf area index. Chamber-  
53 based GPP estimates closely matched those from Eddy Covariance measurements. On an annual  
54 scale, *F. albida* trees contributed approximately ~~23%~~ ~~50%~~ of total ecosystem GPP, with a carbon  
55 use efficiency of 0.48. Net annual ~~vertical~~ CO<sub>2</sub> exchange was estimated at  $-1.4 \pm 0.4602$  and  $-1.8$   
56  $\pm 0.1704$  Mg C-CO<sub>2</sub> ha<sup>-1</sup> using chamber and Eddy Covariance methods, respectively. These  
57 findings underscore the role of *F. albida*-based agroforestry systems as effective carbon sinks in  
58 Sahelian landscapes, supporting their potential contribution to climate change mitigation.

59 **Keywords:** Sahelian agro-silvo-pastoral systems, CO<sub>2</sub> fluxes, automated static chambers, Eddy  
60 Covariance, 'fertile island effect' ~~of trees~~, carbon ~~balances~~ ~~budgets~~.

61 **1. Introduction**

62 Plant photosynthesis and respiration —both autotrophic (plant) and heterotrophic (microbial)—  
63 are fundamental processes driving carbon dioxide (CO<sub>2</sub>) fluxes in terrestrial ecosystems  
64 (Lambers et al., 2008; Raich et al., 2014; Reichle, 2020). Accurate quantification of these processes  
65 is critical for assessing ecosystem carbon (C) sink potential (Baldocchi, 2020), particularly for  
66 informing climate-smart land management strategies.

67 To capture these processes at the ecosystem scale, the Eddy Covariance (EC) technique has  
68 emerged as a transformative method, enabling continuous and high-frequency CO<sub>2</sub> flux  
69 measurements (Baldocchi, 2003, 2008). The EC technique quantifies CO<sub>2</sub> exchanges between  
70 ecosystems and the atmosphere by correlating fluctuations in vertical wind velocity with  
71 simultaneous variations in CO<sub>2</sub> concentrations, providing a direct and non-invasive estimate of  
72 CO<sub>2</sub> fluxes (Baldocchi, 2003). Extensive EC networks in Europe (Stojanović et al., 2024), Asia (Yu  
73 et al., 2011), and the Americas (Chu et al., 2021) have significantly advanced our understanding  
74 of the global C cycle. In contrast, sub-Saharan Africa remains critically underrepresented  
75 (Bombelli et al., 2009; Houghton & Hackler, 2006; Williams et al., 2007). Although some studies  
76 have used EC (Ardö et al., 2008; Brümmner et al., 2008; Merbold et al., 2009; Tagesson et al., 2016),  
77 static chambers (Assouma et al., 2017; Owusu et al., 2024; Rosenstock et al., 2016; Wachiye et al.,  
78 2020), or modeling approaches (Agbohessou et al., 2023, 2024; Delon et al., 2019; Rahimi et al.,  
79 2021), they remain sparse and methodologically heterogeneous, limiting comparability and  
80 regional C budget integration.

81 Among these underrepresented landscapes, agroforestry systems in the Sahel— particularly  
82 agro-silvo-pastoral systems (ASPS) that combine trees, crops, and livestock— are increasingly  
83 promoted for sustainable land management and climate resilience (Cardinael et al., 2021; Gupta  
84 et al., 2023; Mbow et al., 2014; Stetter & Sauer, 2024). However, the structural and functional  
85 heterogeneity of these systems poses significant challenges for accurately quantifying and  
86 upscaling C fluxes. *Faidherbia albida*, a keystone agroforestry tree species in these ASPs (Leroux  
87 et al., 2022; Lu et al., 2022), is of particular interest due to its reverse phenology, capacity to  
88 enhance soil fertility and crop yields (Bayala et al., 2020; Roupsard et al., 2020; Sileshi et al., 2016;  
89 2020). Yet, its functional role in modulating both the magnitude and seasonal dynamics of CO<sub>2</sub>  
90 fluxes remains poorly understood.

91 Addressing this knowledge gap requires integrated approaches capable of capturing both  
92 aggregate and component-specific CO<sub>2</sub> fluxes. While EC remains the gold standard method for CO<sub>2</sub>  
93 flux measurements at the landscape scale (Baldocchi, 2003), it captures net ecosystem exchange  
94 (NEE) as an aggregate signal, without separating the contributions from individual compartments  
95 such as soil, crops, and trees. This limits its utility for disentangling processes and attributing  
96 sources in heterogeneous systems like ASPs. Automatic static chambers provide a valuable

a mis en forme : Indice

a mis en forme : Indice

a mis en forme : Indice

97 complement to EC, as they enable continuous, high-frequency measurements at finer scales and  
98 at the level of specific ecosystem components. This approach facilitates component-specific  
99 quantification of CO<sub>2</sub> fluxes, particularly from soil and crop compartments (Luo & Zhou, 2006;  
100 Denmead, 2008; Zaman et al., 2021). When combined with EC, this dual-method approach  
101 strengthens source attribution and improves the partitioning upscaling of fluxes across complex  
102 agroforestry landscapes.

103 This study presents one of the first integrated quantification of CO<sub>2</sub> fluxes in a Sahelian ASPS  
104 dominated by *F. albida*, combining EC and automatic static chambers.

105 Specifically, we the study aims to (1) conduct year-round, high-frequency *in situ* CO<sub>2</sub> flux  
106 measurements from soil and crops using automated static chambers; (2) partition the net CO<sub>2</sub>  
107 fluxes (FCO<sub>2</sub>ch) into respiration (Rch) and photosynthesis (GPPch); (3) investigate the  
108 environmental drivers of fluxes and the spatial variability linked to tree presence; and (4)  
109 compare chamber-based flux estimates with ecosystem-scale measurements derived from the EC  
110 method.

111 Based on these objectives, we hypothesize that (1) Rch and GPPch are higher under the canopy of  
112 *F. albida* than in full sun, (2) soil moisture is the main environmental factor directly controlling  
113 both Rch and GPPch, (3) when extrapolated to the field scale, the chamber-based method provides  
114 seasonal dynamics of respiration and photosynthesis fluxes comparable to those derived from EC  
115 technique.

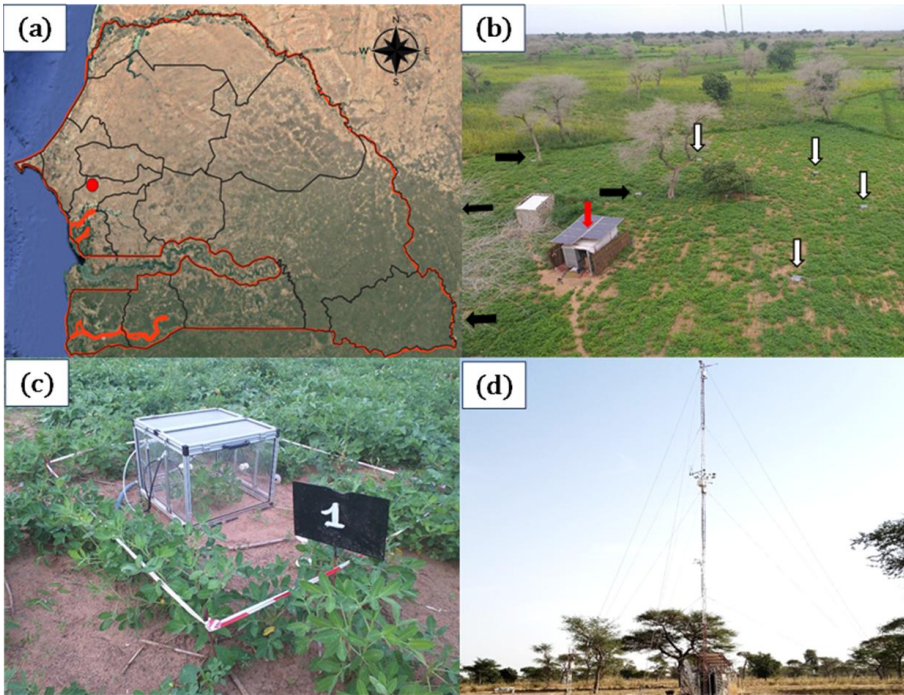
116 **2. Materials and methods**

117 *2.1. Site description*

118 The study was conducted in the agroforestry parkland of Sob village (Niakhar municipality, Fatick  
119 region), located in the groundnut basin of Senegal, within the Sahelo-Sudanian climatic zone of  
120 West Africa (Fig. 1). The climate is characterized by a long dry season (8–9 months) with high  
121 temperatures and strong diurnal variations, and a short rainy season from late June to mid-  
122 October (Delaunay et al., 2018).

123 Soils are locally known as "*Dior*" and classified as Arenosols (IUSS Working Group WRB, 2022).  
124 The topsoil has low organic matter (<1%) and phosphorus (<3 mg kg<sup>-1</sup>), a sandy texture (>85%  
125 sand), and an acidic pH (Malou et al., 2021; Siegwart et al., 2022). Rainfed agriculture  
126 predominates. The main cropping system includes pearl millet (*Pennisetum glaucum L.*) and  
127 groundnut (*Arachis hypogaea L.*) in biennial rotation, with occasional intercropping of cowpea  
128 (*Vigna unguiculata L.*).

129 The site hosts the 'Faidherbia Flux' station (14°29'44.916"N; 16°27'12.851"W; FLUXNET ID: SN-  
130 Nkr), a long-term research platform for monitoring ecosystem services in agroforestry systems.  
131 It is dominated by *F. albida*, a nitrogen-fixing, reverse-phenology tree with deep roots accessing  
132 groundwater (Roupsard et al., 1999). The tree density is ~13 trees ha<sup>-1</sup>, with canopies covering  
133 ~10% of the soil surface (Roupsard et al., 2020). The EC tower is installed at 20 m height,  
134 approximately 12.5 m above the canopy. The study field is a typical 'bush field', characterized by  
135 low soil fertility, no mineral fertilization, and off-site export of crop residues and manure (Malou  
136 et al., 2021).



137 Fig. 1: Study area.

138 (a) geographical location of Sob, Groundnut basin, Senegal (Map data © Google Earth, 2025), (b) overview  
 139 (image from the Eddy Covariance tower located in the same bush-field) of the *Faidherbia albida* parkland  
 140 during the rainy season, depicting groundnut crops with bare soil in the inter-row, *F. albida* trees  
 141 (defoliated during the rainy season, average height = 13m) and location of the chambers under the Shade  
 142 of trees (horizontal black arrows; N=4) and in Full sun (vertical white arrows; N=4); The shelter (red  
 143 arrow) with solar panels is to fit the analyser, automation and batteries (c) automatic chamber enclosing a  
 144 groundnut plant (during the rainy season) or bare soil (during the dry season), (d) Eddy Covariance (EC)  
 145 tower (measurement height = 20 m) during the dry season.

146 2.2. *Experimental setup*

147 2.2.1. *CO<sub>2</sub> flux measurements in automatic chambers*

148 Continuous net CO<sub>2</sub> fluxes (FCO<sub>2</sub>ch) from soil and groundnut plants were measured over a full  
149 phenological year (June 17, 2021 – June 17, 2022) using eight automated static chambers  
150 (50×50×50 cm), each enclosing one groundnut plant. Four chambers were installed in full sun  
151 (FS), at least 20 m from trees, and four under *F. albida* canopy shade (Sh). The chambers were  
152 transparent, custom-built (Duthoit et al., 2020), and installed on metal bases embedded 10 cm  
153 into the soil one month prior to measurements.

154 During the rainy season (June–November), groundnut coexisted briefly with spontaneous weeds  
155 until weeding (mid-July), after which chambers contained only groundnut. Post-harvest (early  
156 November), chambers remained bare while surrounding plots experienced weed regrowth.

157 CO<sub>2</sub> concentrations were measured at 1 Hz using a Picarro G2508 gas analyser (Picarro Inc., Santa  
158 Clara, CA, USA) (Fleck et al., 2013; Reum et al., 2019; Valujeva et al., 2022). A fully automated  
159 system was built for sequential half-hour flux measurements (alternating FS and Sh  
160 chambers) (S1, Table S1.2). Measurement duration was 15 min per chamber in the dry season,  
161 reduced to 5 min during the rainy season to limit condensation effects.

162 2.2.2. *CO<sub>2</sub> flux measurements by Eddy Covariance*

163 The EC system (Li-COR SMARTFLUX®, including a Gill MasterPro 3D sonic anemometer and a LI-  
164 7500 RS open path CO<sub>2</sub> and H<sub>2</sub>O gas analyser) was mounted at a height of 20 m on a 30m mast,  
165 above *F. albida*. It continuously monitored net CO<sub>2</sub> exchange from the ecosystem. Raw data were  
166 collected at 20 Hz frequency and post-processed from binary files using the advanced mode of the  
167 EddyPro® v7.0, with standard corrections and procedures: sonic tilt correction (double rotation),  
168 block averaging, covariance maximisation for time lag, and WPL correction (Webb et al., 1980).  
169 Quality control followed Foken et al. (2004) and Vickers & Mahrt (1997); random uncertainty was  
170 estimated per Finkelstein & Sims (2001). Spectral corrections were applied according to  
171 Moncrieff et al. (1997, 2004). Footprints were computed according to Kormann and Meixner  
172 (2001), using the FREddyPro R package (Xenakis, 2016), indicating indicated a ~1 ha source area  
173 covering the entire field. Gap-filling and flux partitioning were conducted using ReddyProc  
174 (Wutzler et al., 2018), applying the daytime partitioning approach of Lasslop et al. (2010).

175 2.2.3. *Ancillary measurements*

176 Environmental and vegetation variables were monitored continuously throughout the study.  
177 Global radiation (R<sub>g</sub>) was estimated from photosynthetically active radiation (PAR) using a Skye  
178 sensor (averaged over 30-min intervals). [The normalised difference vegetation index \(NDVI\)](#) of

179 crops under full sun was recorded semi-hourly by a calibrated downward-facing sensor installed  
180 at 20 m height (Pontailier et al., 2003), processed following Soudani et al. (2012), and used to  
181 estimate [the leaf area index \(LAI\)](#) time series for groundnut, weeds, and cowpea based on end-of-  
182 season field LAI measurements in six 15 m<sup>2</sup> plots (as in Roupsard et al., 2020).

183 Rainfall was recorded by an automatic weather station (CR1000 with TE525MM rain gauge,  
184 Campbell Scientific), and soil volumetric water content (VWC) and temperature (T<sub>soil</sub>, at 6 cm  
185 depth) were monitored using TOMST® TMS-4 sensors, benchmarked prior to field deployment  
186 inside and outside the chambers (Wild et al., 2019). Air temperature (T<sub>air</sub>) was recorded inside  
187 each chamber at 15 cm above ground, all at 5-min intervals. These measurements contribute to  
188 the SoilTemp global database (Lembrechts et al., 2020, 2022).

189 Groundnut development was tracked weekly by counting leaves in each chamber. Total  
190 groundnut LAI (LAI<sub>ch</sub>) was then derived from average single-leaf area and chamber surface.

191 A detailed description of the data used in this study is provided in Supplement S1 (Table S1.1).

### 192 2.3. Data processing

#### 193 2.3.1. Flux calculation

194 Net CO<sub>2</sub> fluxes (FCO<sub>2ch</sub>, in μmol CO<sub>2</sub> m<sup>-2</sup> s<sup>-1</sup>) from the chambers were calculated from the linear  
195 change in CO<sub>2</sub> concentration over time (ΔC/Δt; [Fig. S1.1.](#)) using the Eq.1.

$$196 \text{FCO}_{2\text{ch}} = \left(\frac{P}{RT_k}\right) \left(\frac{V}{A}\right) \left(\frac{\Delta C}{\Delta t}\right) \quad (\text{Eq. 1})$$

197 where P is atmospheric pressure (101 325 N m<sup>-2</sup>), R is the ideal gas constant (8.31 N m mol<sup>-1</sup> K<sup>-1</sup>),  
198 T<sub>k</sub> is air temperature inside the chamber in Kelvin, V (0.125 m<sup>3</sup>) is the total system volume  
199 (chamber, tubing, analyser cavity, pump, and water trap), and A (0.25 m<sup>2</sup>) is the chamber  
200 footprint. The slope ΔC/Δt was obtained via linear regression (Duthoit et al., 2020).

201 Mean FCO<sub>2ch</sub> values were computed separately for the four replicate chambers in full sun (FS)  
202 and under *F. albida* shade (Sh). By convention, negative values indicate net CO<sub>2</sub> uptake  
203 (photosynthesis), and positive values indicate net CO<sub>2</sub> release (respiration).

#### 204 2.3.2. Quality control of chamber-based CO<sub>2</sub> flux measurements

205 The quality of chamber-based CO<sub>2</sub> flux measurements was assessed using [a threshold of the](#)  
206 [coefficient of determination \(R<sup>2</sup> ≥ 0.8\)](#) of the linear increase in CO<sub>2</sub> concentration during chamber  
207 closure. The minimum detectable flux (MDF) was then calculated following Nickerson (2016)  
208 (Eq.2). The MDF defines the flux detection threshold, below which data are considered unreliable  
209 due to instrument sensitivity and sampling constraints (Zaman et al., 2021). In this study, the MDF  
210 was ±0.0004 μmol CO<sub>2</sub> m<sup>-2</sup> s<sup>-1</sup>.

211 
$$\mathbf{MDF} = \left( \frac{A_a}{t_c(\sqrt{t_c/p_s})} \right) \left( \frac{VP}{ART} \right) \quad \mathbf{(Eq. 2)}$$

212 where  $A_a$  is the analytical precision of the Picarro analyser (0.6 ppm; Picarro Inc., 2015),  $t_c$  the  
213 closure time (s),  $p_s$  the sampling frequency (1 Hz),  $V$  the chamber volume,  $P$  the atmospheric  
214 pressure (101 325 N m<sup>-2</sup>),  $A$  the chamber footprint,  $R$  the gas constant (8.3 N m mol<sup>-1</sup>·K<sup>-1</sup>), and  $T$   
215 the air temperature in Kelvin.

216 Following this quality control, fluxes were partitioned (Section 2.3.3) and gap-filled (Section  
217 2.3.4).

### 218 *2.3.3. Partitioning of chamber-based CO<sub>2</sub> fluxes*

219 The net CO<sub>2</sub> fluxes (FCO<sub>2</sub>ch), averaged from four chambers per environment (FS and Sh), were  
220 partitioned into two components according to Eq. 3 (Reichstein et al., 2005).

221 
$$\mathbf{FCO_2ch} = \mathbf{Rch} + \mathbf{GPPch} \quad \mathbf{(Eq. 3)}$$

222 Rch includes heterotrophic respiration (Rh) from soil and other autotrophic respiration (Ra) from  
223 groundnut plants and roots of *F. albida* (Ra Groundnut + Ra tree below-ground). Rch is always  
224 positive (Rch > 0). GPPch (Gross Primary Productivity) represents the photosynthetic CO<sub>2</sub> uptake  
225 by the groundnut plants and is negative during the day (GPPch < 0), and zero at night, when  
226 FCO<sub>2</sub>ch = Rch.

227 Half-hourly FCO<sub>2</sub>ch fluxes were partitioned as follows: (1) an Arrhenius-type function (Lloyd &  
228 Taylor, 1994) was fitted between nocturnal Rch and T<sub>soil</sub> during nighttime periods, for each 5-days  
229 throughout the time series (Eq. 4). This empirical formulation is based on several key  
230 assumptions. First, the relationship between nocturnal respiration and soil temperature is  
231 assumed to follow an exponential response, reflecting the temperature sensitivity of respiration  
232 processes. Second, the model assumes temporal stability of the respiration–temperature  
233 relationship between night and day, allowing diurnal respiration to be extrapolated from fitted  
234 parameters in Eq.4 and daytime T<sub>soil</sub>. Third, we assumed that no abrupt changes in substrate  
235 availability or soil moisture occur between day and night — conditions that could otherwise  
236 disrupt the temperature–respiration relationship. ~~Third, it is assumed that no abrupt changes in~~  
237 ~~substrate availability or soil moisture occur between night and day — conditions that could~~  
238 ~~otherwise decouple respiration rates from temperature.~~ These assumptions are widely applied in  
239 CO<sub>2</sub> flux partitioning approaches (Reichstein et al., 2005; Lasslop et al., 2010). (2) Diurnal Rch  
240 was estimated by applying the Lloyd & Taylor function, previously calibrated on nocturnal data,  
241 to the corresponding daytime T<sub>soil</sub> measurements for each 5-day interval. (3) GPPch was  
242 subsequently derived as the residual component of the net CO<sub>2</sub> flux during the day, according to:

243 **nocturnal Rch** =  $R_{\text{ref}} \cdot \exp \left[ E_0 \left( \frac{1}{T_{\text{ref}} - T_0} - \frac{1}{T_{\text{soil}} - T_0} \right) \right]$  (Eq. 4)

244 where  $R_{\text{ref}}$  ( $\mu\text{mol CO}_2 \text{ m}^{-2} \text{ s}^{-1}$ ) is a fitted parameter representing the base respiration at the  
 245 reference temperature [ $T_{\text{ref}}$  (K), (set at 288.15 K)].  $E_0$  (K) is the temperature sensitivity (set at  
 246 250 K),  $T_{\text{soil}}$  (K) the soil temperature (K), and  $T_0$  (K) is kept constant at 231.13 K, according to  
 247 Lloyd & Taylor (1994).

248 **GPPch** = **diurnal FCO<sub>2</sub>ch** – **diurnal Rch** (Eq. 5)

249 where diurnal FCO<sub>2</sub>ch and diurnal Rch represent the daytime net CO<sub>2</sub> fluxes and respiration in  
 250  $\mu\text{mol CO}_2 \text{ m}^{-2} \text{ s}^{-1}$ , respectively.

#### 251 2.3.4. Gap-filling procedure

252 Missing Rch data were gap-filled using the model derived from Eq. 4 (Lloyd & Taylor, 1994). Prior  
 253 to gap-filling GPPch, raw data were standardised by LAI to reduce variability between chambers  
 254 due to differences in leaf surface area (Eq. 6). A light-response model was then fitted to the  
 255 standardised GPPch data, every 5-day period, to gap-fill missing values. The model is based on a  
 256 rectangular hyperbolic function that describes the relationship between photosynthetic CO<sub>2</sub>  
 257 uptake and incoming global radiation (Rg) (Eq. 7). It corresponds to a Michaelis–Menten-type  
 258 light-response curve, commonly used in ecosystem carbon exchange studies (Falge et al., 2001;  
 259 Lasslop et al., 2010).

260 **GPPch.stand** =  $\frac{\text{GPPch}}{\text{LAIch}} * \text{LAI.field}$  (Eq. 6)

261 where GPPch.stand ( $\mu\text{mol CO}_2 \text{ m}^{-2} \text{ s}^{-1}$ ) is the standardised GPPch. LAIch and LAI.field ( $\text{m}^2$  leaves  
 262  $\text{m}^{-2}$  soil) represent the groundnut LAI inside the chambers and the groundnut + weeds + cowpea  
 263 LAI for the whole field, respectively.

264 **GPP** =  $\frac{\alpha\beta Rg}{\alpha Rg + \beta}$  (Eq. 7)

265 where  $\alpha$  ( $\mu\text{mol CO}_2 \text{ J}^{-1}$ ) represents the light use efficiency of the groundnut plants inside the  
 266 chambers, and refers to the initial slope of the light-response curve,  $\beta$  ( $\mu\text{mol CO}_2 \text{ m}^{-2} \text{ s}^{-1}$ ) is the  
 267 maximum CO<sub>2</sub> uptake rate by the groundnut plants at light saturation, and Rg the global radiation  
 268 ( $\text{W m}^{-2}$ ).

#### 269 2.3.5. Comparing chamber-based (Ch) and Eddy Covariance (EC) methods

270 Chamber measurements were upscaled to field-level CO<sub>2</sub> fluxes and compared with EC-derived  
 271 fluxes. Before comparison, a correction was applied (Eq. 6) to account for differences in LAI  
 272 between chambers (LAIch) and the field (LAI.field), due to the presence of cowpea and weeds in  
 273 the field but not in the weeded chambers.

274 Upscaling considered tree cover, with FS and Sh chamber fluxes weighted at 90% and 10%,  
 275 respectively. Rch.stand and GPPch.stand, representing chamber-based respiration and

276 photosynthesis at field scale. These fluxes were compared, on a half-hourly basis, to EC-derived  
277 Reco.EC and GPP.EC (S3, Table S3.1). The November–December transition period was excluded  
278 due to weed-driven uncertainties after groundnut harvest.

279 During the rainy season (*F. albida* leafless), GPP.EC represented ground vegetation (groundnut,  
280 cowpea, weeds), while Reco.EC included autotrophic respiration from all vegetation (including  
281 trees), and heterotrophic respiration (Reco.EC =  $R_a$  tree below-ground +  $R_a$  tree above-ground  
282 +  $R_a$  groundnut +  $R_a$  cowpea +  $R_a$  weeds +  $R_h$ ). Rch.stand could not be fully upscaled to the field  
283 due to uncertainty in its partitioning between  $R_a$  and  $R_h$ . Rch.stand accounted only for  $R_a$  tree  
284 below-ground,  $R_a$  groundnut, and  $R_h$ .

285 In the dry season (leafy trees, bare soil), GPP.EC reflected tree photosynthesis only (GPP tree),  
286 while GPPch.stand was nil. Reco.EC included  $R_a$  tree (above- and below-ground) and  $R_h$ .  
287 Rch.stand, measured on bare soil, represented only  $R_a$  tree below-ground +  $R_h$ .

### 288 2.3.6. Contribution of trees to full ecosystem respiration and photosynthesis

289 During the dry season, when the trees (*F. albida*) maintained their foliage, a comparison between  
290 chamber and EC measurements allowed for the estimation of the contribution of the above-  
291 ground tree compartments to total ecosystem respiration (S3, Table S3.1). Based on this estimate,  
292 total tree respiration ( $R_a$  tree) was then calculated under the assumption that the tree root  
293 systems ( $R_a$  tree below-ground) represent  $\frac{1}{3}$  of the above-ground biomass (Jackson et al. 1996).  
294 Given the GPP measured during the dry season was equivalent to GPP of trees (GPP trees) from  
295 EC measurements, the carbon use efficiency of the trees (CUE tree) was then calculated (S3, Table  
296 S3.1). The resulting CUE value was assessed to determine whether it approximated the typical  
297 value of 0.5, which is often used as a default in ecosystem models (Zhou et al., 2019; 2020).

### 298 2.3.7. Net annual vertical C balance budget at the ASPS scale

299 The net annual C balance budget of CO<sub>2</sub> fluxes in a yearly basis was estimated for chambers and  
300 EC measurements in Mg C-CO<sub>2</sub> ha<sup>-1</sup>. The chambers CO<sub>2</sub> flux balances fluxes budgets were  
301 obtained by calculating the annual sum of the net CO<sub>2</sub> flux measurements and then weighting with  
302 the tree cover rate (10% for the Sh, 90% for the FS). These annual budgets balances for the field  
303 are considered apparent representing vertical CO<sub>2</sub> exchanges only, as they do not account for the  
304 biomass exported from the field after the harvest, the decomposition of which therefore escaped  
305 both the chambers and the EC. Additionally, the inputs and the outputs of fecal matter resulting  
306 from livestock wandering during the dry season were not quantified and are therefore neglected.  
307 The objective here is to compare two approaches at different scales using apparent-vertical net C  
308 budgets balances, rather than to provide an absolute C budget which would also include horizontal  
309 transfers of carbon.

a mis en forme : Indice

310 2.4. Statistical analyses

311 Statistical analyses were performed using the R software (R. Core Team, 2023). To compare the  
312 mean values of climatic parameters between the FS and Sh situations, a non-parametric Mann-  
313 Whitney test was used when both the normality (shapiro.test) and the homogeneity of the  
314 variance (Levene Test, R package 'Car'; Fox et al., 2023) were not confirmed. This approach was  
315 similarly applied to compare the seasonal dynamics of CO<sub>2</sub> fluxes between FS and Sh, as well as  
316 between the chamber-based and Eddy Covariance (EC) methods. Means and standard deviations  
317 were computed using the 'skim' function from the R package 'skimr' (Waring et al., 2022).

318 Respiration (R<sub>ch</sub>) (Eq. 4) and GPP (GPP<sub>ch</sub>) models (Eq. 7) were fitted using non-linear least  
319 squares regression, implemented in the library in R 'nls.multstart' (Padfield et al., 2025). For the  
320 GPP<sub>ch</sub> model, parameters  $\alpha$  and  $\beta$  with non-significant p-values were removed, and then the  
321 remaining values were interpolated and smoothed using a 'spline' function from the 'zoo' library  
322 in R (Zeileis et al., 2024). Ordinary least-square linear regressions were fitted between the  
323 measured and the modeled values derived from. Model performance of Eq. 4 and Eq. 7 was  
324 evaluated by fitting ordinary least-square linear regressions between the measured and the  
325 modeled values using R<sup>2</sup>, root mean square error (RMSE), and the bias metrics. Given that the  
326 primary objective of these equations was to accurately reproduce the seasonal dynamics of the  
327 CO<sub>2</sub> fluxes to fill gaps in data, particular emphasis was placed on R<sup>2</sup>, with a higher value reflecting  
328 a better fit of the model to the measurements.

329 Correlation analysis was conducted between chamber CO<sub>2</sub> fluxes (FCO<sub>2</sub>ch, R<sub>ch</sub>, GPP<sub>ch</sub>) and soil  
330 temperature (T<sub>soil</sub>, °C), air temperature (T<sub>air</sub>, °C), VWC, the leaf area index of groundnut plants in  
331 the chambers (LAI<sub>ch</sub>), and the fitted parameters for respiration — R<sub>ref</sub> — and photosynthesis —  
332  $\alpha$  and  $\beta$ . This analysis was performed using the 'cor.test' function from the 'stats' package in R  
333 (Lüdecke et al., 2021), applying the Spearman method.

334 The threshold of the daily mean soil temperature (T<sub>soil</sub>, °C) at which the cumulative daily  
335 respiration (R<sub>ch</sub>, g C-CO<sub>2</sub> m<sup>-2</sup> d<sup>-1</sup>) began to decline was determined using segmented regression  
336 from the R package 'segmented' (Muggeo, 2003). The associated uncertainty (standard error) of  
337 this estimate was evaluated through a bootstrap procedure.

338 The standard error of the total annual flux was estimated using the error propagation method.  
339 This calculation considered the mean standard deviation of daily fluxes (g C-CO<sub>2</sub> d<sup>-1</sup>) and the  
340 effective number of measurement days (365). For each FS and Sh condition, the mean daily  
341 standard deviation was multiplied by the square root of 365 to obtain the annual standard error.  
342 The resulting values were then weighted by 90% for FS and 10% for Sh to derive the overall  
343 standard error of the annual flux sum, which was subsequently converted to Mg C-CO<sub>2</sub> ha<sup>-1</sup>.

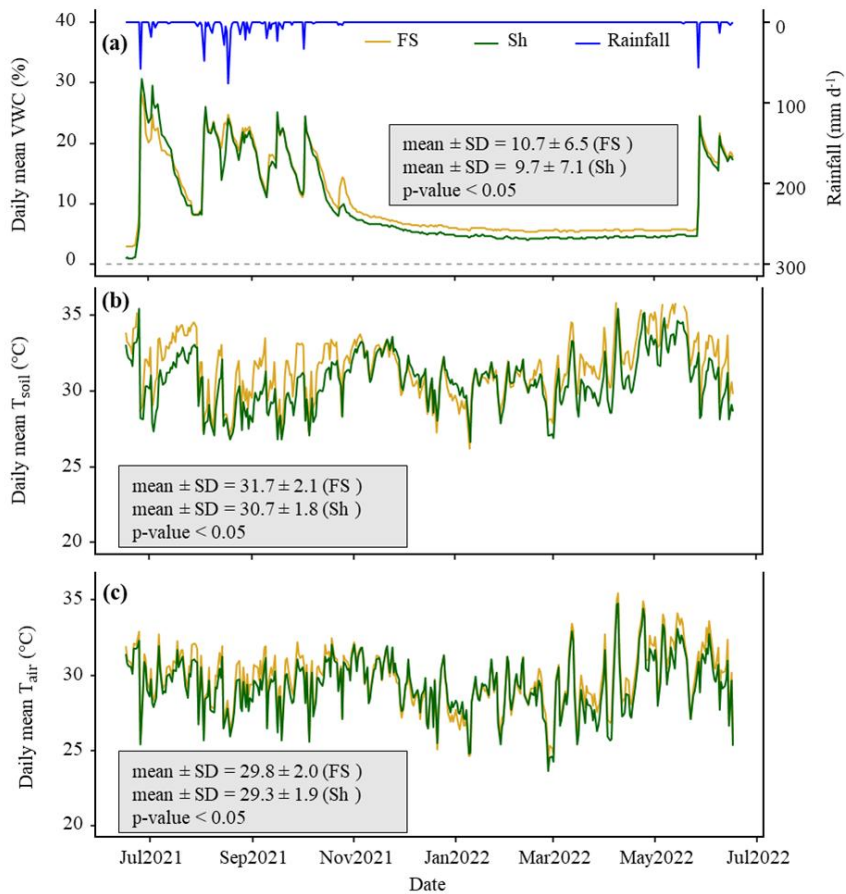
a mis en forme : Espace Après : 0 pt

### 344 3. Results

#### 345 3.1. Microclimatic conditions

346 During the experiment, the cumulative rainfall was 550 mm, which was representative of the  
347 interannual average. Precipitations were lowest in July and highest between August and  
348 September, a period that typically corresponds to the peak of the rainy season (Fig. 2a). Global  
349 radiation ranged between 5.8 and 32.4 MJ m<sup>-2</sup> d<sup>-1</sup> (data not shown). The daily mean VWC in the  
350 chambers showed significant variation, ranging from 1% at the end of the dry season to a  
351 maximum of 30% during the rainy season (Fig. 2a). While VWC was similar during the rainy  
352 season, it remained consistently higher in FS than in Sh throughout the dry season ( $p < 0.05$ ),  
353 which was unexpected. However, it should be noted that the last rain of October 2021 recharged  
354 the FS chambers more effectively, likely due to foliage rainfall interception by *F. albida* which had  
355 just put on leaves at that time, potentially explaining this discrepancy in VWC.

356 Within the chamber, the daily mean  $T_{\text{soil}}$  ranged from 26°C in April to 37.5°C at the end of the dry  
357 season (Fig. 2b), while  $T_{\text{air}}$  varied between 23.7°C and 35.5°C (Fig. 2c). However, during  
358 instantaneous daily peaks,  $T_{\text{soil}}$  could exceed 45°C in May (data not shown). As expected, both daily  
359 mean  $T_{\text{soil}}$  and  $T_{\text{air}}$  were significantly higher in FS compared to Sh situations ( $p < 0.05$ ), with  $T_{\text{soil}}$   
360 and  $T_{\text{air}}$  averaging respectively 1°C and 0.5°C lower under the tree canopy.



361 Fig. 2: One-year time series of daily average microclimatic parameters measured inside [the](#)  
 362 chambers.

363 (a) volumetric soil water content (VWC) at a depth of 6 cm (%). (b) soil temperature ( $T_{soil}$ ) at a depth of 6  
 364 cm ( $^{\circ}C$ ), (c) air temperature ( $T_{air}$ ) at a height of 15 cm ( $^{\circ}C$ ). The blue line depicts the daily rainfall ( $mm\ d^{-1}$ )  
 365 throughout the year. FS: Full sun chambers; Sh: Shaded chambers. Mean and SD represent respectively the  
 366 mean value and the standard deviation. The p-value indicates the probability associated with the statistical  
 367 test, assessing the differences in means between FS and Sh with the significance level  $\alpha$  set to 0.05.

368 3.2. Modeling the chamber-based total respiration ( $R_{ch}$ ) and photosynthesis ( $GPP_{ch}$ )

369 3.2.1. Dynamics of reference respiration, light use efficiency, and maximum  $CO_2$  uptake rate at  
370 light saturation ( $R_{ref}$ ,  $\alpha$ , and  $\beta$ )

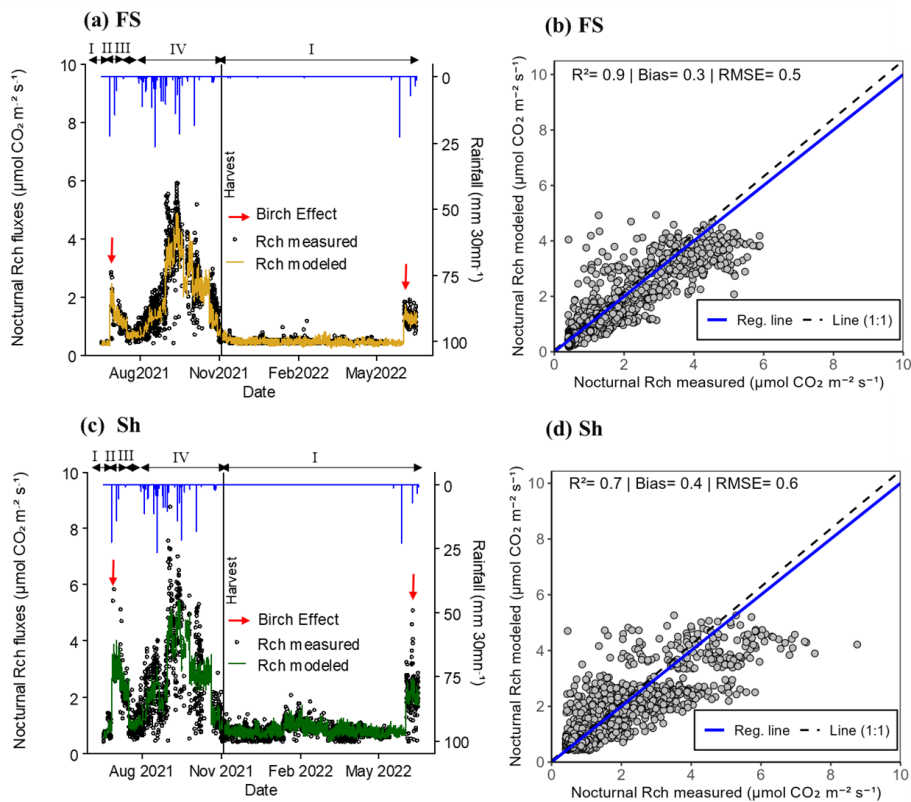
371 The reference respiration ( $R_{ref}$ ) showed comparable seasonal dynamics both at a distance from  
372 the trees (FS) and under the tree canopies (Sh) (S2, Fig. S2.2). In both situations,  $R_{ref}$  showed  
373 strong variability during the rainy season, peaking in September 2021 at  $2.4 \mu\text{mol CO}_2 \text{ m}^{-2} \text{ s}^{-1}$  for  
374 FS and  $2.9 \mu\text{mol CO}_2 \text{ m}^{-2} \text{ s}^{-1}$  for Sh (S2, Table S2.1). In contrast, during the dry season — from  
375 November 3, 2021 (after harvest) until the onset of the following rainy season (June 2022) —  $R_{ref}$   
376 values dropped both for FS and Sh, averaging  $0.3 \pm 0.5 \mu\text{mol CO}_2 \text{ m}^{-2} \text{ s}^{-1}$  for FS and  $0.5 \pm 0.6 \mu\text{mol}$   
377  $\text{CO}_2 \text{ m}^{-2} \text{ s}^{-1}$  for Sh. This represents a reduction by a factor of 8 for FS and 6 for Sh compared to the  
378 rainy season. The mean annual  $R_{ref}$  values were significantly higher under Sh than in FS, with value  
379 approximately 1.5 times greater (S2, Table S2.1).

380 Regarding GPP in chambers, the light use efficiency ( $\alpha$ ) and the maximum  $CO_2$  uptake by  
381 groundnut plants in the chambers ( $\beta$ ), also reached their maximum during the peak of the rainy  
382 season (S2, Fig. S2.3, a and b). The maximum value of  $\alpha$  reached  $0.2 \mu\text{mol CO}_2 \text{ J}^{-1}$  in FS and  $0.3$   
383  $\mu\text{mol CO}_2 \text{ J}^{-1}$  in Sh (S2, Table S2.1). Similarly, the maximum values of optimum  $CO_2$  uptake rate at  
384 light saturation ( $\beta$ ) were  $40.2 \mu\text{mol CO}_2 \text{ m}^{-2} \text{ s}^{-1}$  for FS and  $42.8 \mu\text{mol CO}_2 \text{ m}^{-2} \text{ s}^{-1}$  for Sh (S2, Table  
385 S2.1). In the dry season, when photosynthetic activity ceased in the chambers, both  $\alpha$  and  $\beta$  were  
386 assumed to be nil (S2, Fig. S2.3, a and b). On average,  $\alpha$  and  $\beta$  were significantly higher in Sh than  
387 in FS, by a factor of 1.7 and 1.2, respectively (S2, Table S2.1). We noted that the decline in  
388 photosynthetic activity of the groundnut crop occurred earlier and rapidly at a distance from the  
389 trees (FS), as reflected by the sharply observed recession of  $\alpha$  and  $\beta$  in FS.

390 3.2.2. Dynamics of nocturnal respiration in chambers

391 The averaged nocturnal respiration (nocturnal  $R_{ch}$ ) calculated from the measurements across  
392 each treatment (FS and Sh), showed similar seasonal patterns (Fig. 3, a and c). Following the first  
393 rains,  $R_{ch}$  values increased dramatically, with a nocturnal 'Birch effect' — a sudden pulse of  $CO_2$   
394 release following soil rewetting — observed to be more pronounced under Sh compared to FS,  
395 approximately by a factor of 2. At the peak of the rainy season (September), the maximum  
396 nocturnal  $R_{ch}$  values reached approximately  $6.0 \mu\text{mol CO}_2 \text{ m}^{-2} \text{ s}^{-1}$  in FS and  $9.0 \mu\text{mol CO}_2 \text{ m}^{-2} \text{ s}^{-1}$   
397 in Sh (Fig. 3, a and c). Thereafter, nocturnal  $R_{ch}$  declined well before the groundnut harvest along  
398 with the rainfall spacing and the groundnut crop senescence (data not shown). During the dry  
399 season nocturnal  $R_{ch}$  continued to decrease, with maximum values around  $1.0 \mu\text{mol CO}_2 \text{ m}^{-2} \text{ s}^{-1}$   
400 in FS and  $2.0 \mu\text{mol CO}_2 \text{ m}^{-2} \text{ s}^{-1}$  in Sh (Fig. 3, a and c).

401 The modeled nocturnal Rch values closely matched the measured nocturnal Rch values (mean  
402 across four chambers per treatment), as indicated by the model performance metrics ( $R^2 = 0.9$ ,  
403 with bias and RMSE values of 0.3 and 0.5  $\mu\text{mol CO}_2 \text{ m}^{-2} \text{ s}^{-1}$ , respectively, for FS;  $R^2 = 0.7$ , with bias  
404 and RMSE values of 0.4 and 0.6  $\mu\text{mol CO}_2 \text{ m}^{-2} \text{ s}^{-1}$ , respectively, for Sh) (Fig. 3, b and d). Similarly,  
405 the daily mean modeled values also fitted well with the measured values, with FS showing (mean  
406 + standard deviation)  $0.9 \pm 0.9 \mu\text{mol CO}_2 \text{ m}^{-2} \text{ s}^{-1}$  (modeled) and  $1.2 \pm 1.2 \mu\text{mol CO}_2 \text{ m}^{-2} \text{ s}^{-1}$   
407 (measured), while Sh recorded  $1.4 \pm 0.9 \mu\text{mol CO}_2 \text{ m}^{-2} \text{ s}^{-1}$  (modeled) and  $1.5 \pm 1.2 \mu\text{mol CO}_2 \text{ m}^{-2}$   
408  $\text{s}^{-1}$  (measured). Given the close match between the measured and modeled values, the fitted  
409 model parameters were used subsequently to fill data gaps and estimate diurnal Rch values, as  
410 presented in Fig. 4, a and c.



411 Fig. 3: Dynamics of instantaneous nocturnal CO<sub>2</sub> fluxes in chambers in Full sun (FS; a and b) and  
 412 Shaded (Sh; c and d) environments (data filtered based on R<sup>2</sup> of the CO<sub>2</sub> variation over the time  
 413 of chamber closure and Minimum Detectable Flux, Eq.2).

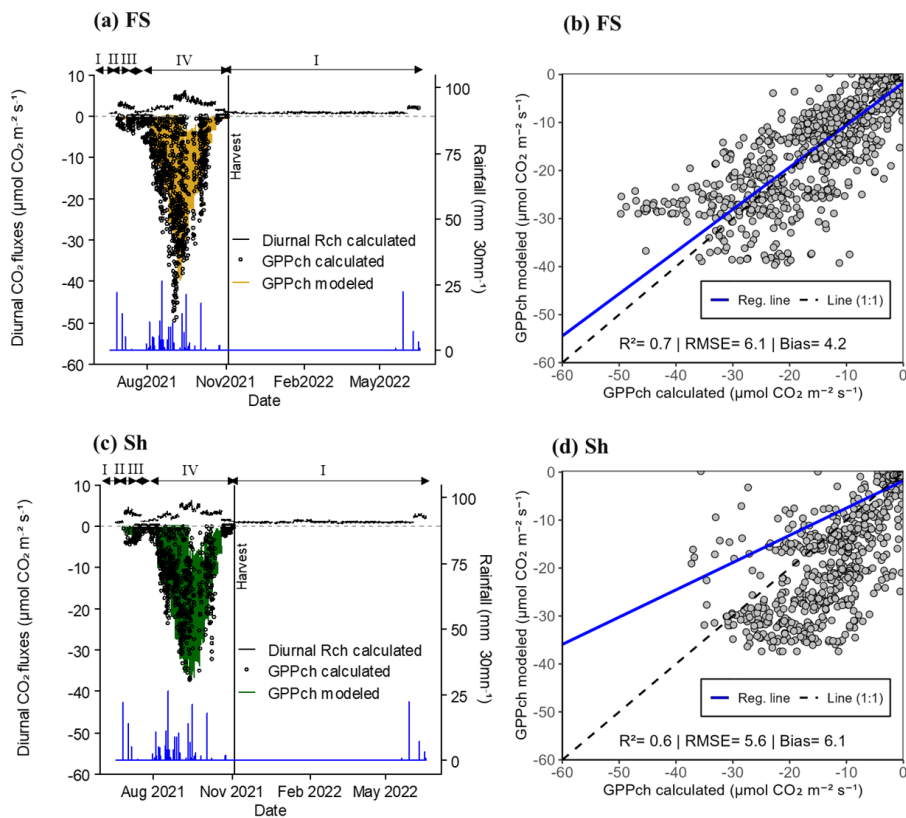
414 (a) and (c): measured nocturnal respiration in chambers (Rch: black dots; average of measurements in 4  
 415 chambers per location) vs. modeled (coloured line). The vertical black line indicates the harvest date of  
 416 groundnuts inside the chambers. The red arrows indicate the 'Birch' effect and the blue line represents the  
 417 rainfall (mm 30mn<sup>-1</sup>). Roman numerals (above the black arrows) refer to vegetation conditions prevailing  
 418 inside the chambers, i.e. (I) bare soil, (II) weeds, (III) weeds + groundnuts, and (IV) groundnuts only.  
 419 (b) and (d): scatter plot between measured and modeled nocturnal Rch. The solid blue line indicates the  
 420 regression line and the dashed black one the (1:1) line RMSE and bias are expressed as fluxes (in μmol CO<sub>2</sub>  
 421 m<sup>-2</sup> s<sup>-1</sup>). Each point represents the mean value from 4 chambers within the FS or Sh environments.

422 3.2.3. Dynamics of daytime fluxes in chambers

423 The measured GPPch.stand, as well as GPP modeled with Eq. 6, showed similar seasonal dynamics  
424 inFS and Sh (Fig. 4, a and c). The fluxes peaked during the rainy season (Fig. 4a and c), coinciding  
425 with periods of vigorous vegetative growth characterised by a high leaf area index (LAIch) of  
426 groundnut plants within the chambers (S2, Fig. S2.1). The maximum calculated and standardised  
427 GPPch values reached  $-50 \mu\text{mol CO}_2 \text{ m}^{-2} \text{ s}^{-1}$  for FS and  $-37 \mu\text{mol CO}_2 \text{ m}^{-2} \text{ s}^{-1}$  for Sh. As expected,  
428 these fluxes were nil during the dry season when the soil was bare (Fig. 4, a and c).

429 The modeled GPPch values closely followed the same trends as the calculated values, although  
430 model performance was slightly better for FS ( $R^2 = 0.7$  with bias and RMSE values of 4.2 and 6.1  
431  $\mu\text{mol CO}_2 \text{ m}^{-2} \text{ s}^{-1}$ , respectively) compared to Sh ( $R^2 = 0.6$  with bias and RMSE values of 6.1 and  
432  $5.6 \mu\text{mol CO}_2 \text{ m}^{-2} \text{ s}^{-1}$ , respectively) (Fig. 4, b and d).

433 The calculated diurnal respiration values (diurnal Rch calculated) for FS and Sh revealed a 'Birch  
434 effect' similar to that observed during the night, though slightly more pronounced under Sh by a  
435 factor of 1.2. Diurnal Rch values increased significantly during the rainy season, reaching a  
436 maximum of  $6.0 \mu\text{mol CO}_2 \text{ m}^{-2} \text{ s}^{-1}$  for both FS and Sh (Fig. 4, a and c). In the dry season, on bare  
437 soil, these values declined, with maximum respiration reaching only  $0.5 \mu\text{mol CO}_2 \text{ m}^{-2} \text{ s}^{-1}$  for both  
438 situations (FS and Sh) (Fig. 4, a and c).



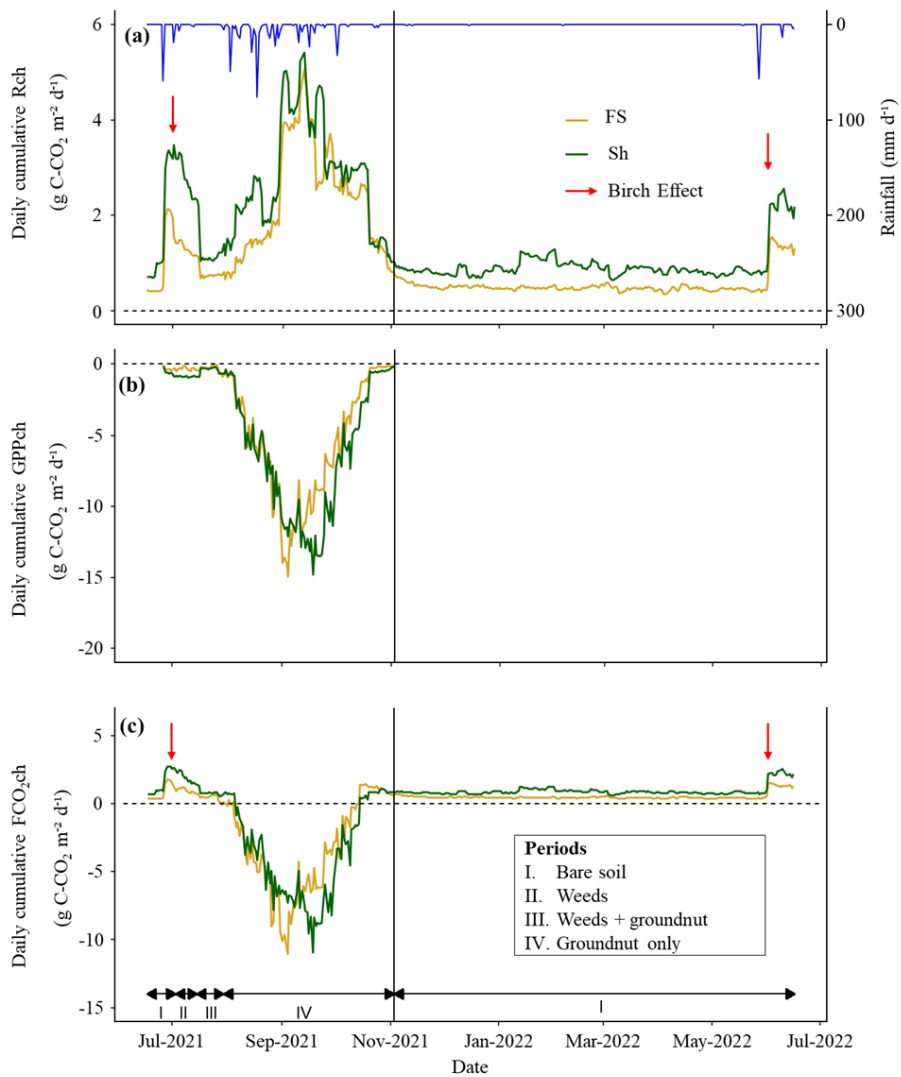
439 Fig. 4: Dynamics of instantaneous diurnal CO<sub>2</sub> fluxes in chambers in Full sun (FS; a and b) and  
 440 Shaded (Sh; b and d) environments (filtered based on R<sup>2</sup> of the CO<sub>2</sub> variation over the time closure  
 441 in FS and Sh and Minimum Detectable Flux, Eq.2).

442 (a) and (c): non-gap-filled diurnal Rch calculated (black line, positive values; average of measurements in  
 443 4 chambers per location) and GPPch calculated from Eq.5 then standardised for LAI (black dots, negative  
 444 values) and modeled (coloured line, negative values). The vertical black line indicates the harvest date of  
 445 groundnuts inside the chambers and the blue line represents the rainfall (mm 30mn<sup>-1</sup>). Roman numerals  
 446 (above the black arrows) refer to conditions prevailing inside the chambers, i.e., (I) bare soil, (II) weeds,  
 447 (III) weeds + groundnuts, and (IV) groundnuts.

448 (b) and (d): scatter plot between calculated and modeled GPPch. The solid blue line indicates the regression  
 449 line and the dashed black one the (1:1) line. RMSE and bias are expressed as fluxes (in µmol CO<sub>2</sub> m<sup>-2</sup> s<sup>-1</sup>).  
 450 Each point represents the mean value from 4 chambers within the FS or Sh environments.

451 3.3. Dynamics of daily cumulative CO<sub>2</sub> fluxes in chambers

452 The seasonality of daily cumulative of GPPch.stand showed similar dynamics between FS and Sh,  
453 with higher variability during the rainy season than during the dry season (Fig. 5). Daily total Rch  
454 peaked during the rainy season at 5.1 g C-CO<sub>2</sub> m<sup>-2</sup> d<sup>-1</sup> for FS and 5.4 g C-CO<sub>2</sub> m<sup>-2</sup> d<sup>-1</sup> for Sh, while  
455 the maximum GPPch.stand values were comparable at around -15.0 g C-CO<sub>2</sub> m<sup>-2</sup> d<sup>-1</sup> for both FS  
456 and Sh (Table 1; S2, Fig. S2.54, a, b, c, and d). In the dry season, Rch decreased (Fig. 5), averaging  
457 0.5 g C-CO<sub>2</sub> m<sup>-2</sup> d<sup>-1</sup> for FS and 1.0 g C-CO<sub>2</sub> m<sup>-2</sup> d<sup>-1</sup> for Sh. GPPch declined well before harvest  
458 (senescence) and remained nil during the dry season (Fig. 5). During the rainy season FCO<sub>2</sub>ch  
459 peaked in absolute value at around 11.0 g C-CO<sub>2</sub> m<sup>-2</sup> d<sup>-1</sup> for FS and Sh (Fig. 5) (Table 1; S2, Fig.  
460 S2.54, e and f), while FCO<sub>2</sub>ch values were the same as Rch during the dry season. In absolute terms,  
461 the mean Rch and GPPch were significantly higher under Sh as compared to FS, by factors of 1.3  
462 and 1.2, respectively. Conversely, the mean FCO<sub>2</sub>ch was significantly higher in absolute value  
463 under FS (0.4 g C-CO<sub>2</sub> m<sup>-2</sup> d<sup>-1</sup>) than under Sh (0.2 g C-CO<sub>2</sub> m<sup>-2</sup> d<sup>-1</sup>) (Table 1).  
464 The annual cumulative Rch values were 392.8 g C-CO<sub>2</sub> m<sup>-2</sup> for FS and 574.5 g C-CO<sub>2</sub> m<sup>-2</sup> for Sh.  
465 The GPPch fluxes reached -539.5 g C-CO<sub>2</sub> m<sup>-2</sup> for FS and -632.6 g C-CO<sub>2</sub> m<sup>-2</sup> for Sh. The net Annual  
466 net cumulative C exchange (FCO<sub>2</sub>ch) were was -146.7 g C-CO<sub>2</sub> m<sup>-2</sup> in FS and -58.1 g C-CO<sub>2</sub> m<sup>-2</sup> in  
467 Sh.



468 Fig. 5: Seasonal dynamics of daily gap-filled cumulative fluxes (in  $\text{gC-CO}_2 \text{ m}^{-2} \text{ d}^{-1}$ ) in chambers.

469 (a) soil+crop respiration (Rch), (b) photosynthesis (GPPch, standardised for LAI) and (c) net  $\text{CO}_2$  exchange  
 470 ( $\text{FCO}_{2\text{ch}}$ ). The yellow and green solid lines compare the FS and Sh environments, respectively. The vertical  
 471 black line indicates the harvest date of groundnuts inside the chambers. The blue line depicts the daily  
 472 cumulative rainfall ( $\text{mm d}^{-1}$ ) throughout the rainy season, and the red arrow indicates the 'Birch'  
 473 effect. Roman numerals (above the black arrows) in (a) and (c) refer to the prevailing conditions inside the  
 474 chambers: (I) bare soil, (II) weeds, (III) weeds + groundnuts, (IV) groundnuts.

475 Table 1: Comparison of daily cumulative and gap-filled chamber CO<sub>2</sub> fluxes (Rch, GPPch  
 476 standardised for LAI, and FCO<sub>2</sub>ch in g C-CO<sub>2</sub> m<sup>-2</sup>) in the FS and Sh condition.  
 477

	Annual sum	Daily Mean ±SD	Min	Max	Mann-Whitney test
(g C-CO <sub>2</sub> m <sup>-2</sup> )	.yr <sup>-1</sup>	.d <sup>-1</sup>	.d <sup>-1</sup>	.d <sup>-1</sup>	
<b>Rch</b>					
FS	392.8	1.1 ± 0.9	0.4	5.1	*
Sh	574.5	1.6 ± 1.1	0.6	5.4	
<b>GPPch</b>					
FS	-539.5	-4.1 ± 4.3	< -0.1	-14.9	*
Sh	-632.6	-4.8 ± 4.6	< -0.1	-14.8	
<b>FCO<sub>2</sub>ch</b>					
FS	-146.7	-0.4 ± 2.4	-11.0	1.8	*
Sh	-58.1	-0.2 ± 2.7	-10.9	2.8	

478 Annual sum corresponds to the annual cumulative fluxes (g C-CO<sub>2</sub> m<sup>-2</sup> yr<sup>-1</sup>). Mean, SD, Min, and Max  
 479 represent respectively the mean, standard deviation, minimum, and maximum values at the daily scale (g  
 480 C-CO<sub>2</sub> m<sup>-2</sup> d<sup>-1</sup>). Asterisks (\*) indicate the p-values from the Mann-Whitney test, used to assess differences in  
 481 mean between FS and Sh (p < 0.05). Positive values indicate CO<sub>2</sub> emissions, while negative values represent  
 482 CO<sub>2</sub> uptake.

483 3.4. Drivers of daily respiration and photosynthesis in chambers

484 The chamber-based daily cumulative respiration (Rch) and GPPch showed significant and positive  
485 correlations with the leaf area index (LAIch), both at a distance from the trees (FS) and under the  
486 trees (Sh) (Table 2). The influence of LAIch on GPPch was stronger ( $r = 0.86$  for FS and Sh) than  
487 its influence on Rch ( $r = 0.60$  for FS;  $r = 0.69$  for Sh). Soil VWC was also positively correlated with  
488 Rch and GPPch, both in FS and Sh. However, the influence of soil VWC on Rch was stronger under  
489 Sh compared to FS, while its influence on GPPch was similar in both situations (FS and Sh). Soil  
490 temperature showed weak negative correlations with Rch (in FS and Sh) and with GPPch (only in  
491 Sh). Finally, no significant correlations were found between  $T_{air}$ , and any of the  $CO_2$  fluxes (Table  
492 2).

493 Table 2: Spearman correlation matrix based on daily cumulative and gap-filled CO<sub>2</sub> fluxes from full  
 494 year chamber measurements (g C-CO<sub>2</sub> m<sup>-2</sup> d<sup>-1</sup>) with microclimatic parameters.

Parameters	Condition	r-coef. Rch	p (Rch)	r-coef. GPPch	p (GPPch)
T <sub>soil</sub>	FS	-0.25 ***	<u>7.47 x 10<sup>-4</sup></u>	ns	<u>1.18 x 10<sup>-3</sup></u>
	Sh	-0.28 ***	<u>9.69 x 10<sup>-14</sup></u>	-0.38 ***	<u>2.88 x 10<sup>-7</sup></u>
T <sub>air</sub>	FS	ns	<u>0.22</u>	ns	<u>0.35</u>
	Sh	ns	<u>0.98</u>	ns	<u>0.15</u>
VWC	FS	0.51 ***	<u>3.00 x 10<sup>-34</sup></u>	0.75 ***	<u>6.73 x 10<sup>-3</sup></u>
	Sh	0.78 ***	<u>1.29 x 10<sup>-66</sup></u>	0.75 ***	<u>0.02</u>
LAIch	FS	0.60 ***	<u>1.11 x 10<sup>-61</sup></u>	0.86 ***	<u>2.23 x 10<sup>-8</sup></u>
	Sh	0.69 ***	<u>6.08 x 10<sup>-69</sup></u>	0.86 ***	<u>2.11 x 10<sup>-12</sup></u>

a mis en forme le tableau

495 Spearman correlation coefficients (r-coef) between daily cumulative and gap-filled CO<sub>2</sub> flux components  
 496 (Rch and GPPch, with GPPch in absolute terms) and daily mean microclimatic parameters in full sun (FS)  
 497 and shaded chambers (Sh). T<sub>soil</sub> (°C) is the daily mean soil temperature at 6 cm depth, T<sub>air</sub> (°C) the daily  
 498 mean air temperature at 15 cm height, VWC (%) the daily mean volumetric water content (VWC, %), and  
 499 LAIch (m<sup>-2</sup> leaf m<sup>-2</sup> soil) the chamber leaf area index value for a given day. Letter p represents the p-value  
 500 and significance levels are indicated by (\*\*\*) p<0.001; \*\* p<0.01; \* p<0.05 for p<0.001; ns denotes a non-  
 501 significant correlation (p > 0.05).

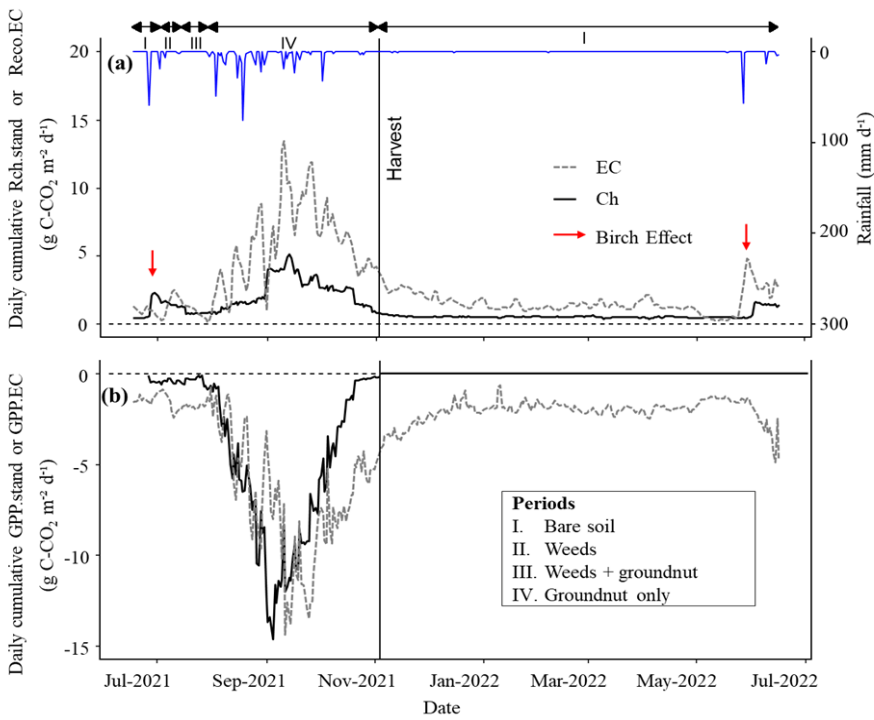
502 3.5. Comparison of respiration and GPP measurements between chambers (Ch) and Eddy  
503 Covariance (EC) methods

504 The chamber-based daily total CO<sub>2</sub> fluxes, gap-filled and weighted according tree cover were  
505 compared with the fluxes obtained using the EC method (Fig. 6).

506 During the rainy season, both total respiration and GPP showed comparable dynamics between  
507 the two methods, with synchronised peaks and higher variability compared to the dry season (Fig.  
508 6). The maximum value of Reco.EC, peaked at 13.5 g C-CO<sub>2</sub> m<sup>-2</sup> d<sup>-1</sup> (Table 3). The initial value of  
509 Rch.stand was comparable to Reco.EC but peaked only at 5.1 g C-CO<sub>2</sub> m<sup>-2</sup> d<sup>-1</sup> (Table 3), meaning  
510 a third of the peak of Reco.EC. The maximum GPP, was -14.3 g C-CO<sub>2</sub> m<sup>-2</sup> d<sup>-1</sup> and -14.6 g C-CO<sub>2</sub>  
511 m<sup>-2</sup> d<sup>-1</sup> for GPP.EC and GPPch.stand, respectively (Table 3). This indicates that the LAI-based  
512 standardisation and upscaling approach were realistic, at least up to the peak of groundnut  
513 growth.

514 On average, Reco.EC was significantly higher than Rch.stand, by a factor of 2.3. GPP.EC was also  
515 significantly higher than GPPch.stand, but only by a factor of 1.2 (Table 3).

516 During the dry season, Reco.EC and Rch.stand gradually decreased. The values for Reco.EC  
517 remained higher than for Rch.stand, which was fairly consistent with the contribution of the Ra  
518 tree above-ground compartment, even if this difference seemed to disappear at the end of the dry  
519 season (Fig. 6). The measured 'Birch effect' was highest for Rch.stand in 2021, but was the  
520 opposite in 2022 due to a system failure at the beginning of the rainy season. The maximum value  
521 of GPP.EC reached -2.4 g C-CO<sub>2</sub> m<sup>-2</sup> d<sup>-1</sup> when the trees were at their maximum of foliage, after  
522 harvest and while weeds were still present in the field. However, after the harvest, chamber  
523 photosynthesis (GPPch.stand) was nil (Table 3).



524 Fig 6: Comparing the seasonal dynamics of CO<sub>2</sub> fluxes between Eddy Covariance (EC)  
 525 measurements and upscaled chamber measurements (ch.stand).

526 (a) represent the seasonal dynamics of soil + crop respiration (Rch.stand) and ecosystem respiration  
 527 (Reco.EC) and (b) photosynthesis (GPP.stand and GPP.EC). The black and dashed grey lines show Ch and  
 528 EC seasonal dynamics, respectively. The vertical black line indicates the harvest date of groundnuts inside  
 529 the chambers. The blue line depicts the daily cumulative rainfall (mm d<sup>-1</sup>), and the red arrow indicates the  
 530 'Birch' effect. Roman numerals (above the black arrows) refer to conditions prevailing inside the  
 531 chambers: (I) bare soil, (II) weeds, (III) weeds + groundnuts, (IV) groundnuts.

532 Table 3: Comparison of gap-filled CO<sub>2</sub> fluxes between Eddy Covariance (EC) and upscaled chamber (Ch.stand) measurements, by season (rainy or dry).

	Rainy season				Dry season			
	Daily Mean ± SD	Min	Max	Mann-Whitney test	Daily Mean ± SD	Min	Max	Mann-Whitney test
(g C-CO <sub>2</sub> m <sup>-2</sup> )	.d <sup>-1</sup>	.d <sup>-1</sup>	.d <sup>-1</sup>		.d <sup>-1</sup>	.d <sup>-1</sup>	.d <sup>-1</sup>	
<b>Reco.EC or Rch.stand</b>								
EC	4.6 ± 3.2	0.2	13.5	*	1.2 ± 0.4	0.3	2.1	*
Ch.stand	2.0 ± 1.1	0.5	5.1		0.5 ± 0.04	0.4	0.6	
<b>GPP.EC or GPPch.stand</b>								
EC	-5.1 ± 3.6	-0.7	-14.3	*	-1.7 ± 0.3	-0.6	-2.4	
Ch.stand	-4.2 ± 4.3	<-0.1	-14.6		0	0	0	

533 Mean, SD, Min, and Max represent the daily mean fluxes, standard deviation, minimum, and maximum values, respectively (g C- CO<sub>2</sub> m<sup>-2</sup> d<sup>-1</sup>). The Asterisks (\*) indicate  
534 the p-values from the Mann-Whitney test, used to assess differences in mean between EC and Ch. Positive values indicate CO<sub>2</sub> emissions, while negative values  
535 represent CO<sub>2</sub> uptake.

536 3.6. *The contribution of F. albida to Reco and GPP*

537 During the dry season, the cumulative contribution of *F. albida* to ecosystem respiration (Ra tree)  
538 was 139.6 g C-CO<sub>2</sub> m<sup>-2</sup>. This represent ~~14%~~~~12%~~ of the total annual cumulative Reco, which was  
539 estimated at ~~1000.0~~~~1180.0~~ g C-CO<sub>2</sub> m<sup>-2</sup> (S3, Table S3.1). The contribution of trees (GPP tree) to  
540 total annual GPP in absolute term was -270.2 g C-CO<sub>2</sub> m<sup>-2</sup>, equivalent to ~~~23%~~~~50%~~ of the total  
541 annual cumulative GPP of the ecosystem measured by EC (~~1180.0~~~~550~~ g C-CO<sub>2</sub> m<sup>-2</sup>) (S3, Table  
542 S3.1).

543 The ratio between these two components (Ra tree / GPP tree) in absolute terms was 0.52,  
544 reflecting a carbon use efficiency (CUE) of 0.48 (S3, Table S3.1).

545 3.7. Annual vertical CO<sub>2</sub> balances~~Carbon budgets~~ at the field-scale

546 The upscaled chamber-based annual cumulative total respiration flux (Rch.stand) was estimated  
547 to be 4.1 ± 0.~~1801~~ Mg C-CO<sub>2</sub> ha<sup>-1</sup> (Table 4). In comparison, the annual ~~budget of~~ Reco.EC was 10.0  
548 ± 0.~~4903~~ Mg C-CO<sub>2</sub> ha<sup>-1</sup> (Table 4), more than two times larger than Rch.stand.

549 The upscaled GPPch.stand reached an annual cumulative value of -5.5 ± 0.~~8303~~ Mg C-CO<sub>2</sub> ha<sup>-1</sup>,  
550 whereas the annual cumulative GPP.EC was -11.8 ± 0.~~5303~~ Mg C-CO<sub>2</sub> ha<sup>-1</sup> (Table 4).

551 The net annual vertical net C budgetbalance, based on both methods, was estimated at -1.4 ±  
552 0.~~4602~~ Mg C-CO<sub>2</sub> ha<sup>-1</sup> for chambers (FCO<sub>2</sub>ch.stand) and -1.8 ± 0.~~1701~~ Mg C-CO<sub>2</sub> ha<sup>-1</sup> for Eddy  
553 Covariance (NEE.EC) (Table 4).

a mis en forme : Indice

554 Table 4: Annual budget of CO<sub>2</sub> fluxes based on Eddy Covariance (EC) and upscaled chamber  
 555 methods (Ch.stand).

	Annual sum (Mg C-CO <sub>2</sub> ha <sup>-1</sup> )	Std error (Mg C-CO <sub>2</sub> ha <sup>-1</sup> )
<b>Reco.EC or Rch.stand</b>		
EC	10.0	<del>0.4903</del>
Ch.stand	4.1	<del>0.1801</del>
<b>GPP.EC or GPPch.stand</b>		
EC	-11.8	<del>0.5303</del>
Ch.stand	-5.5	<del>0.8303</del>
<b>NEE.EC or FCO<sub>2</sub>ch.stand</b>		
EC	-1.8	<del>0.1701</del>
Ch.stand	-1.4	<del>0.4602</del>

556 Annual sum corresponds to the annual cumulative fluxes for full year measurements (Mg C-CO<sub>2</sub> ha<sup>-1</sup>). EC  
 557 refers to fluxes measured by the Eddy Covariance method, and Ch refers to the fluxes measured by  
 558 chambers, which are then upscaled to the whole field. Rch.stand represents the chamber respiration, while  
 559 Reco.EC denotes the ecosystem respiration according to the EC method. GPP.EC and GPPch.stand are the  
 560 gross primary production or photosynthesis flux, measured by EC and Ch methods, respectively. NEE.EC  
 561 and FCO<sub>2</sub>ch.stand represent the net ecosystem exchange for EC and Ch, respectively. The associated  
 562 standard error is denoted as Std error (Mg C-CO<sub>2</sub> ha<sup>-1</sup>). Positive values indicate CO<sub>2</sub> emissions, while  
 563 negative values represent CO<sub>2</sub> uptake.

## 564 4. Discussion

### 565 4.1. Soil respiration modeling and limitations regarding the temperature

566 In this study the Lloyd and Taylor (1994) model, based on a modified Arrhenius-type formulation,  
567 was used to model nocturnal soil respiration fluxes for estimating daytime respiration. Unlike the  
568 classical Arrhenius equation, this model includes the  $(T_{\text{soil}} - T_0)$  term in the denominator of the  
569 exponential expression (Eq. 4), which inherently limits the effects of high temperatures by  
570 progressively reducing the temperature sensitivity of soil respiration as temperatures rise above  
571 a given threshold. This structural feature produces a flattening of the respiration-temperature  
572 relationship at elevated temperatures, thereby preventing the overestimations (Lloyd and Taylor,  
573 1994).

574 The Lloyd and Taylor model has successfully been widely applied, primarily in boreal and  
575 temperate ecosystems (Lasslop et al., 2010; Reichstein et al., 2003), and relies on the assumption  
576 of comparable thermal conditions between daytime and nighttime periods (Juszczak et al., 2012).  
577 In our study, instantaneous soil temperatures ranged from 20.7 to 45.8 °C during the day and from  
578 22.1 to 45.0 °C at night, indicating largely overlapping thermal ranges between the two periods.  
579 Model parameters were recalibrated using five-day fixed windows, which provided sufficient  
580 temporal resolution while capturing seasonal dynamics of soil respiration.

581 This study represents one of the first applications of the Lloyd and Taylor model in a Sahelian  
582 semi-arid context. While Arrhenius based models are known to potentially overestimate fluxes  
583 under extreme temperatures due to physiological limitations, over the range of temperatures  
584 observed in this study, the modeled soil respiration was not overestimated (Fig. S2.4). Thus, the  
585 model used in this study appears to provide a realistic representation of soil respiration under  
586 local conditions. However, this conclusion is site-specific and should not be interpreted as a  
587 general validation of temperature-based models across all semi-arid environments. Such models  
588 should be systematically validated with respect to temperature to ensure their reliability.

### 589 4.1.4.2. Seasonality and drivers of chamber-based CO<sub>2</sub> fluxes

590 In our agroforestry context, seasonal variability in CO<sub>2</sub> fluxes closely followed rainfall dynamics,  
591 peaking during the wet season and declining sharply in the dry season, consistent with soil  
592 moisture depletion and crop senescence. This pattern is typical of semi-arid ecosystems (Ago et  
593 al., 2016a; Brümmer et al., 2008; Guillen-Cruz et al., 2023; Macharia et al., 2020; Mosongo et al.,  
594 2022; Wieckowski et al., 2024).

595 Respiration and photosynthesis were primarily driven by soil moisture and LAI, reflecting the  
596 system's sensitivity to water availability and crop dynamics. Soil moisture enhanced both  
597 processes by stimulating microbial activity and supporting plant growth (Borken et al., 2002;

598 Conant et al., 2004; Merbold et al., 2009; Yu et al., 2020; Zhao et al., 2016). The stronger correlation  
599 between soil moisture and respiration under ~~*F. albida*~~*F. albida* canopy (Sh:  $r = 0.78$ ) compared to  
600 full sun (FS:  $r = 0.51$ ) suggests greater microbial sensitivity to moisture beneath trees. This likely  
601 reflects enhanced substrate availability, resulting in stronger post-rainfall respiration pulses  
602 (Meisner et al., 2015) and supporting the 'fertile island' effect, where trees improve local soil  
603 conditions (Eldridge et al., 2024). Photosynthetic capacity also responded to soil moisture, as  
604 shown by positive correlations with LAI and key physiological traits such as light use efficiency  
605 ( $\alpha$ ) and maximum CO<sub>2</sub> uptake rate ( $\beta$ ) (Gonsamo et al., 2019; Qiu et al., 2023; Zhang et al., 2024).  
606 In contrast, the influence of soil temperature ( $T_{\text{soil}}$ ) on respiration was weakly negative in both FS  
607 and Sh, indicating a thermal threshold beyond which respiration is suppressed—estimated at  $32$   
608  $\pm 1.5$  °C in FS and  $29.5 \pm 1.9$  °C in Sh (S2, Fig. S2.76, a and b), similar to findings in Eastern Ghana  
609 (Owusu et al., 2024). This inhibition likely results from decreased enzymatic and microbial  
610 activity under combined heat and water stress (Liu et al., 2018; Richardson et al., 2012). In semi-  
611 arid regions, soil respiration often becomes decoupled from temperature due to seasonal  
612 moisture constraints (Jia et al., 2020; Tucker & Reed, 2016; Warren, 2014), with microbial activity  
613 limited during dry periods despite favourable temperatures. This decoupling helps explain the  
614 weak or absent correlation between  $T_{\text{soil}}$  and soil moisture (S2, Fig. S2.65, b), particularly under  
615 Sh ( $r = -0.28$ ). Management practices such as organic inputs can also modulate these dynamics,  
616 adding further variability to soil respiration responses (Meena et al., 2020; Oyonarte et al., 2012;  
617 Rong et al., 2015; Xue & Tang, 2018).

#### 618 *4.2.4.3. Magnitude of chamber-based total CO<sub>2</sub> respiration fluxes*

619 Mean total soil respiration values were consistent with those reported in other low-input  
620 agricultural systems across sub-Saharan Africa (Mapanda et al., 2010; Pelster et al., 2017;  
621 Rosenstock et al., 2016). In full sun (FS), the mean respiration ( $1.0 \pm 0.9$  g C-CO<sub>2</sub> m<sup>-2</sup> d<sup>-1</sup>) closely  
622 matched values measured by Wachiye et al. (2020) in a semi-arid Kenyan field at 1158 m altitude  
623 ( $1.1 \pm 0.1$  g C-CO<sub>2</sub> m<sup>-2</sup> d<sup>-1</sup>). This similarity likely reflects comparable environmental conditions,  
624 including moderate rainfall ( $\sim 550$  mm yr<sup>-1</sup>) and low soil organic carbon and nitrogen contents  
625 ( $<1\%$ ) in the 0–20 cm layer of sandy soil. In contrast, respiration under *F. albida* canopy (Sh:  $1.6$   
626  $\pm 1.1$  g C-CO<sub>2</sub> m<sup>-2</sup> d<sup>-1</sup>) was higher, likely due to additional autotrophic respiration from tree roots  
627 and greater organic inputs beneath the canopy. Nonetheless, this flux remains close to values  
628 observed in low-input sorghum fields on sandy loam soils in eastern Ghana ( $1.7 \pm 1.1$  g C-CO<sub>2</sub> m<sup>-2</sup>  
629 d<sup>-1</sup>), despite higher rainfall (950–1000 mm yr<sup>-1</sup>) in that region (Owusu et al., 2024).  
630 Cumulative annual respiration fluxes fell within the range reported for Sahelian croplands (250–  
631 450 g C-CO<sub>2</sub> m<sup>-2</sup>) (Brümmer et al., 2009) and other sub-Saharan African agricultural systems (Kim  
632 et al., 2016). The cumulative flux under tree cover is similar to that measured in cassava fields in

a mis en forme : Police :italique

633 eastern Tanzania ( $440 \text{ g C-CO}_2 \text{ m}^{-2} \text{ yr}^{-1}$ ), despite the latter receiving higher rainfall ( $\sim 1115 \text{ mm}$   
634  $\text{yr}^{-1}$ ) (Rosenstock et al., 2016). This convergence may stem from comparable soil fertility  
635 constraints, with low soil organic carbon (1–1.7%) and nitrogen contents ( $<0.5\%$ ). In contrast,  
636 the slightly lower cumulative flux in FS may reflect less favourable microclimatic conditions—  
637 such as elevated soil temperatures and increased aridity away from tree cover—limiting  
638 microbial activity (see Section 4.1).

639 Across sub-Saharan Africa, soil respiration fluxes based on static chamber measurements show  
640 high spatial variability, largely shaped by climate and land use. For example, Owusu et al. (2024)  
641 found higher respiration in woodlands ( $3.8 \pm 0.8 \text{ g C-CO}_2 \text{ m}^{-2} \text{ d}^{-1}$ ) and grazed areas ( $2.7 \pm 1.7$ )  
642 than in croplands ( $1.7 \pm 1.1$ ) in humid eastern Ghana. This gradient was linked to differences in  
643 soil moisture and organic matter. Similarly, Rosenstock et al. (2016) reported much higher fluxes  
644 in highland pastures in Kenya ( $3.8\text{--}4.4 \text{ g C-CO}_2 \text{ m}^{-2} \text{ d}^{-1}$ ) compared to cultivated fields in eastern  
645 Tanzania ( $1.2 \pm 0.2$ ), highlighting the role of vegetation cover and soil fertility.

#### 646 [4.3.4.4](#) *Effect of trees on chamber-based soil respiration and photosynthesis*

647 A notable increase in respiration and photosynthesis fluxes was observed under *F. albida* trees  
648 (Sh) compared at a distance from trees (FS). This increase may indicate the potential role of *F.*  
649 *albida* in modulating  $\text{CO}_2$  exchange dynamics (Rch and GPPch) within this agro-silvo-pastoral  
650 system. These results are consistent with preliminary findings from similar environments  
651 (Duthoit et al., 2020).

652 Numerous studies have investigated the effect of tree species on greenhouse gas fluxes,  
653 particularly  $\text{CO}_2$ , revealing significant variations across different ecological contexts (Bréchet et  
654 al., 2021, 2025; Klaus et al., 2024; Mazza et al., 2021; Ramesh et al., 2013; Rheault et al., 2024).  
655 However, the underlying mechanisms by which trees influence these dynamics are not yet fully  
656 understood.

657 In general, agroforestry systems have been well-documented for their ability to provide a range  
658 of ecosystem services (e.g., Assefa et al., 2024; Bado et al., 2021; Kuyah et al., 2019; Rolo et al.,  
659 2023). Specifically, *Faidherbia*-based agroforestry systems may play a crucial role in regulating  
660  $\text{CO}_2$  exchanges between the soil and atmosphere. *F. albida*-based agroforestry systems are  
661 recognized for enhancing both soil organic and mineral fertility (Bayala et al., 2020; Dilla et al.,  
662 2019; Sileshi, 2016; Sileshi et al., 2020; Stephen et al., 2020), mainly through litter accumulation  
663 and direct inputs from livestock excreta under their canopies. Additionally, the extensive roots  
664 system of *F. albida* trees helps concentrate mineral nutrients, contributing to the formation of a  
665 'fertile island' effect under the trees (Siegwart et al., 2022; Eldridge et al., 2024). Moreover, *F.*  
666 *albida* improve water infiltration (Diongue et al., 2023; Faye et al., 2020; Sarr et al., 2023), enhance  
667 soil moisture retention (Clermont-Dauphin et al., 2023) and contribute to reduced soil

668 temperatures (de Carvalho et al., 2021; Lopes et al., 2024; Sida et al., 2018). These changes foster  
669 a more favourable environment for soil microbial activity and crop development (Diack et al.,  
670 2024; Diene et al., 2024; Leroux et al., 2020; Roupsard et al., 2020) under the trees compared to  
671 open areas. Consequently, this likely explains the stronger effect of soil moisture and the leaf area  
672 index of groundnuts on Rch under the trees, resulting in higher total respiration (Table 2). For  
673 photosynthesis, the effect of these parameters was similar in both FS and Sh (Table 2). However,  
674 the significantly higher intensity of GPPch under Sh can be explained by greater light use efficiency  
675 ( $\alpha$ ) and a higher maximum CO<sub>2</sub> uptake rate at light saturation ( $\beta$ ) in this shaded environment. In  
676 agroforestry systems, light use efficiency can at least partially mitigate the reduction in  
677 photosynthetically active radiation under tree canopies (Charbonnier et al., 2017).  
678 Similar results have been observed in different climatic conditions and ecosystems. Gomes et al.  
679 (2016) investigated soil respiration using mobile chambers (LI-8100-102 model) under trees in  
680 coffee-based agroforestry (AF) systems and in the open areas (FS) in Minas Gerais, Brazil. These  
681 studies were conducted with agroecological management practices, such as weeding,  
682 intercropping maize between coffee rows, and mulching. The AF-agroforestry systems exhibited  
683 lower air and soil temperatures (at 5 and 10 cm depth) and higher air and soil humidity compared  
684 to the open areas FS (Gomes et al., 2016). These authors observed greater spatial variability in soil  
685 respiration in agroforestry system AF (34.1%) compared to the open areas FS (24.2%). This  
686 variability was mainly linked with fluctuations in labile carbon and total nitrogen, reflecting more  
687 favourable soil microclimate for microbial activity in agroforestry system AF. In contrast, soil  
688 temperature (10 cm depth) accounted for most of the variability observed in the open areas FS,  
689 where the absence of tree canopy resulted in high soil temperatures and low soil moisture (Gomes  
690 et al., 2016). Likewise, Haren et al. (2010) reported 38% higher soil respiration near large trees  
691 (DBH > 35 cm) in clay-rich Amazonian forests compared to open sites. Interestingly, the  
692 magnitude of CO<sub>2</sub> fluxes was independent of tree species, indicating that canopy effects may  
693 outweigh species-specific traits in some contexts. In our study, *F. albida*'s influence on CO<sub>2</sub> fluxes  
694 aligns with this general pattern observed in tropical agroforestry. However, the mechanisms  
695 linking individual tree species to microbial and physicochemical drivers of CO<sub>2</sub> dynamics remain  
696 insufficiently understood and warrant further investigation (Jevon et al., 2023).

#### 697 4.4.4.5. Birch Effect

698 A rapid increase in soil respiration was observed following the first rainfall events, particularly  
699 under *F. albida*. This phenomenon can be attributed to the lower bulk density of the soil under the  
700 trees (Clermont-Dauphin et al., 2023; Siegwart et al., 2023), which potentially lead to CO<sub>2</sub>  
701 accumulation during the dry season due to higher soil organic matter (SOM) (Siegwart et al.,  
702 2023). Additionally, the sensitivity of microbial communities to subtle variations in soil moisture,

703 compounded by the tree effect, may further explain this phenomenon, as outlined in Sections 4.1  
704 and 4.3. This phenomenon, known as the 'Birch effect' (Birch, 1958), has been reported across  
705 various semi-arid ecosystems in sub-Saharan Africa (Ago et al., 2016b; Fan et al., 2015;  
706 Wieckowski et al., 2024), as well as other semi-arid ecosystems globally (Roby et al., 2022; Yan et  
707 al., 2014; Yu et al., 2020). In these contexts, the 'Birch effect' may result from the displacement of  
708 soil gas phases by the piston effect generated during water infiltration (Singh et al., 2023).  
709 Furthermore, microbial communities in semi-arid environments adopt osmoregulatory  
710 mechanisms to withstand water deficit (Warren, 2014), which is particularly pronounced during  
711 the dry season. This phenomenon reduces soil microbial metabolism (Schimel et al., 2007). Upon  
712 rapid soil rewetting, especially after prolonged dry periods, soil microbial metabolism process is  
713 swiftly reactivated, leading to a transient pulse in respiration and a CO<sub>2</sub> release (Barnard et al.,  
714 2020; Kim et al., 2012; Manzoni et al., 2020; Vargas et al., 2018). Isotopic signatures of soil  
715 respiration provide evidence supporting the hypothesis that these pulses result from the rapid  
716 mineralisation of necromass or osmolytes excreted by microorganisms under drought stress  
717 (Schimel et al., 2007; Unger et al., 2010). Additional factors may amplify the 'Birch effect'. For  
718 instance, drying-rewetting cycles can induce physical disruption of soil aggregates, enhance  
719 oxygen penetration and thereby expose previously protected organic matter to microbial  
720 decomposition (Rabbi et al., 2024). This increases substrate availability and subsequently boosts  
721 soil respiration fluxes.  
722 The magnitude of the 'Birch effect' is modulated by the severity and duration of drought. Thus, at  
723 our study site, given the 8- to 9-month-long dry season, the 'Birch effect' is particularly intense.  
724 Indeed, extended drought periods promote greater accumulation of microbial necromass and  
725 intensify hypo-osmotic stress responses upon rewetting (Singh et al., 2023).

#### 726 [4.5.4.6](#) *Comparing EC and chamber-based methods*

727 Results revealed high seasonal variability, with higher values during the rainy season compared  
728 to the dry season. This seasonal pattern aligns with findings from studies in the Sahel using the  
729 EC method for CO<sub>2</sub> flux measurements (Brümmer et al., 2008; Tagesson et al., 2015; Agbohessou  
730 et al., 2023, Wieckowski et al., 2024). Comparable patterns have ~~also~~ been ~~also~~ documented at the  
731 ecosystem scale in other semi-arid environments (Ago et al., 2014; Archibald et al., 2009; Ardö et  
732 al., 2008; Jia et al., 2020; Quansah et al., 2015; Williams et al., 2009; Zhang, Bi, et al., 2024).  
733 Several comparative studies between chamber and EC methods have reported both congruent  
734 and divergent CO<sub>2</sub> flux estimates (Bastviken et al., 2022; Poyda et al., 2017; Riederer et al., 2014;  
735 J. Tang et al., 2008; Wang et al., 2010). In the present study, ecosystem respiration fluxes during  
736 the rainy season exhibited notable discrepancies measurements between EC (Reco.EC) and  
737 upscaled chamber-based (Rch.stand). This is attributable to differences in the flux components

738 captured by each method. Specifically, Reco.EC included respiration from below- and above-  
739 ground tree parts, crops (groundnuts and cowpeas), weeds, and soil, whereas Rch.stand  
740 accounted only respiration from below-ground tree, groundnut crop, and soil. Therefore, as  
741 expected, Reco.EC ( $4.6 \pm 3.2$  g C-CO<sub>2</sub> m<sup>-2</sup> d<sup>-1</sup>) were significantly higher than Rch.stand ( $2.0 \pm 1.1$  g  
742 C-CO<sub>2</sub> m<sup>-2</sup> d<sup>-1</sup>).

743 For chamber-based GPP measurements, values were standardised (GPP-stand) by the field's leaf  
744 area index (LAI.field). This allowed it to improve comparability with GPP.EC when trees were  
745 leafless in the rainy season. In both cases, GPP accounted only for crops (groundnut and cowpea)  
746 and weeds, as trees were non-photosynthetic in the rainy season. Despite this standardisation,  
747 GPP.EC values ( $-5.1 \pm 3.6$  g C-CO<sub>2</sub> m<sup>-2</sup> d<sup>-1</sup>) were significantly higher than GPPch.stand values ( $-4.2$   
748  $\pm 4.3$  g C-CO<sub>2</sub> m<sup>-2</sup> d<sup>-1</sup>). However, ~~the no divergence~~ **was observed in August, and the intensity of**  
749 **the peak of GPP in September was similar in both methods**~~did not occur on the peak of GPP (which~~  
750 ~~was very similar in both methods)~~, but from the onset of groundnut senescence, when weeds  
751 became the dominant photosynthetic contributors. Thus, during the groundnut growth season,  
752 with leafless *F. albida* trees and almost no weeds, GPP measurements from EC and chambers  
753 generate closely comparable results. Therefore, this provides an initial form of cross-validation  
754 between the two methods. It is important to note that the EC method integrates CO<sub>2</sub> fluxes over a  
755 larger spatial scale, encompassing all ecosystem components (Baldocchi, 2003), while the  
756 chamber method captures fluxes on a smaller scale (i.e., at the 0.25 m<sup>2</sup> scale). This scale disparity  
757 can introduce uncertainties when upscaling chamber-based fluxes to the field, as vegetation  
758 composition within chambers does not represent the EC footprint's average vegetation. This  
759 makes upscaling chamber-based measurements challenging. Nevertheless, the standardisation  
760 we applied on chamber photosynthesis by LAI has been relatively successful.

761 During the dry season, Reco.EC included respiration from below- and above-ground tree parts  
762 (with leaves) and bare soil, while Rch.stand measured only below-ground tree and bare soil  
763 respiration. Consequently, the difference between Reco.EC and Rch.stand was solely attributable  
764 to above-ground tree respiration (Ra tree above-ground). In terms of GPP, chamber  
765 measurements were nil, whereas GPP.EC reflected only GPP trees.

766 The transition period, characterised by groundnut senescence, tree leaf regrowth, and weed  
767 proliferation, introduced further complexity, amplifying method-specific discrepancies. Rch.stand  
768 measurements facilitated the estimation of tree contribution to Reco.EC (Ra tree) and the  
769 verification of the consistency for EC results in terms of carbon use efficiency (CUE), estimated  
770 here at 0.48. This value indicates that nearly 50% of the carbon captured by trees is allocated to  
771 biomass. The CUE estimate here is well comparable to the global average across diverse  
772 ecosystems, climates, and management practices ( $0.49 \pm 0.14$ ) (Tang et al., 2019). Similar CUE  
773 values have been reported for semi-arid grasslands ( $0.46 \pm 0.10$ ), but our value is notably lower

774 than those documented for wetlands ( $0.61 \pm 0.13$ ) (Tang et al., 2019). Overall, these findings  
775 reinforce the plausibility of our assumptions regarding the compartment-~~s~~ contributions to  
776 Reco.EC and Rch.stand, thereby providing a second cross-validation of the EC-Ch comparison.  
777 However, despite a frequently assumed CUE of 0.5 in models, global estimates span a broad range  
778 (0.20 to 0.82), depending on ecosystem type and management practices (DeLucia et al., 2007;  
779 Tang et al., 2019). This underscores the importance of refining carbon flux models to better  
780 represent the biophysical processes governing CO<sub>2</sub> exchange in semi-arid agroforestry systems.  
781 The combined use of EC and chamber methodologies offers a comprehensive perspective on  
782 ecosystem-scale CO<sub>2</sub> flux dynamics, advancing the understanding of carbon cycling in these  
783 environments.

#### 784 *4.6.4.7. Net annual vertical carbon balance ~~carbon exchange budget~~*

785 The net annual vertical carbon balance ~~annual net carbon (C) exchange budget~~ was quantified at  
786  $-1.4 \pm 0.4602$  Mg C-CO<sub>2</sub> ha<sup>-1</sup> with the chamber method and  $-1.8 \pm 0.1701$  Mg C-CO<sub>2</sub> ha<sup>-1</sup> by the  
787 Eddy Covariance (EC), indicating that the studied agro-silvo-pastoral system functions as a net  
788 carbon sink. These findings corroborate the system-~~s~~ potential role in mitigating greenhouse gas  
789 emissions, consistent with previous studies reporting vertical CO<sub>2</sub> flux balances observations in  
790 semi-arid ecosystems (Rahimi et al., 2021; Tagesson et al., 2015; Agbohessou et al., 2023,  
791 Wieckowski et al., 2024).

792 The estimated net C exchange budget-vertical balance is close to the reported mean for Sahelian  
793 ecosystems ( $-1.6 \pm 0.5$  Mg C-CO<sub>2</sub> ha<sup>-1</sup>; Tagesson et al., 2016). The EC-based net C exchange budget  
794 balance ( $-1.8 \pm 0.1701$  Mg C-CO<sub>2</sub> ha<sup>-1</sup>) is also similar to the value of  $-1.9 \pm 0.4$  Mg C-CO<sub>2</sub> ha<sup>-1</sup>  
795 reported for semi-arid savannas of northeastern Benin, despite higher annual rainfall (1495 mm;  
796 Ago et al., 2016b). Furthermore, our EC estimate is close to the average net C exchange reported  
797 for West African terrestrial ecosystems ( $-2.0 \pm 1.5$  Mg C-CO<sub>2</sub> ha<sup>-1</sup>; Ago et al., 2016a).

798 However, estimates from Tagesson et al. (2015) ( $-2.7 \pm 0.07$  Mg C-CO<sub>2</sub> ha<sup>-1</sup>) for a semi-arid  
799 savannah in Dahra, Senegal, located between the 300 mm and 400 mm isohyets, were  
800 comparatively higher. This is potentially attributable to specific characteristics of that specific  
801 savannah site, such as herbaceous vegetation cover during the rainy season, the presence of  
802 evergreen trees, and land management practices linked to pastoral livestock activities (Tagesson  
803 et al., 2016).

804 The net annual C balance C exchange estimates presented in this study are, in fact, apparent fluxes  
805 representing vertical fluxes only, given that they exclude organic matter (OM) imports and, more  
806 critically, exports, introducing uncertainties. Notably, the export of crop residues and direct inputs  
807 from animal excreta —particularly significant in 'bush fields' during the dry season — were not  
808 accounted for. In our case of 'bush field', crop residues are exported to feed livestock, while

809 livestock faeces are collected for use as fuel or manure in 'home fields'. Such practices may lead to  
810 a significant soil organic carbon stocks depletion (Malou et al, 2021), potentially diminishing the  
811 net C budget ( $-1.4 \pm 0.4602$  Mg C-CO<sub>2</sub> ha<sup>-1</sup>) over time and shifting the system closer to carbon  
812 neutrality (Assouma et al., 2019).

813 These results should be contextualized within the broader framework of climate change and semi-  
814 arid ecosystem management. Although agro-silvo-pastoral systems can function as **apparent**  
815 annual carbon sinks, they remain highly sensitive to interannual rainfall variability and escalating  
816 anthropogenic pressures. Sustainable management practices, particularly regarding **C**  
817 **inputs/outputs from the system regarding crop harvest, residues export/exportations, and cattle**  
818 **free manuring, must be taken into account are essential for to confirm maintaining soil mineral**  
819 **fertility and preserving the system's capacity of the system to act as effective a carbon sink,**  
820 **thereby contributing to climate change mitigation.**

#### 821 **4.7.4.8. Limitations of the study**

822 This study benefited from the inverse phenology of *F. albida*, allowing for direct comparison  
823 between chamber-based GPP (GPPch.stand) and ecosystem-level GPP (GPP.EC) during the  
824 leafless period of the trees. However, the system's spatial heterogeneity —common in  
825 agroforestry— posed challenges for accurately partitioning CO<sub>2</sub> fluxes among trees, crops, and  
826 soil. A key limitation was the development of weeds during the late rainy season, which  
827 complicated the attribution of fluxes, particularly during the transitional period. Additionally,  
828 while GPPch was successfully standardised by LAI for upscaling, this was not feasible for  
829 respiration. Respiration integrates both autotrophic and heterotrophic components, which  
830 respond to different drivers and are not directly linked to LAI, limiting the precision of upscaled  
831 Rch.

832 Future improvements should aim to separately quantify respiration sources —tree roots, crops,  
833 and microbial (heterotrophic) respiration— and account explicitly for the weed layer, to refine  
834 flux partitioning in such complex agroforestry systems.

835 **Furthermore, the present study constitutes only an intermediate step delivering a first integrated**  
836 **estimate of the main vertical CO<sub>2</sub> exchanges (photosynthesis, respiration, and net ecosystem**  
837 **exchange) as a base for a forthcoming paper that will present a more comprehensive carbon**  
838 **budget of the ecosystem. Establishing such a carbon budget would require substantial additional**  
839 **data acquisition and poses considerable methodological challenges. In particular, quantifying**  
840 **carbon inputs/outputs associated with free-ranging livestock grazing would be difficult to achieve**  
841 **with acceptable accuracy. It must also be recognised that the system is in a dynamic, non-steady**  
842 **state, characterised by marked inter-annual variability as well as periods of carbon storage and**  
843 **release, which are difficult to constrain empirically except through modeling.**

a mis en forme : Police :Italique

a mis en forme : Anglais (Royaume-Uni)

a mis en forme : Anglais (Royaume-Uni)

a mis en forme : Anglais (Royaume-Uni)

844 **Conclusion**

845 This study demonstrates the successful application of automated static chambers to quantify CO<sub>2</sub>  
846 fluxes in a Sahelian agroforestry system dominated by *F. albida*. The continuous, high-frequency  
847 measurements captured key seasonal dynamics and short-lived events (e.g., Birch effect),  
848 providing a more accurate assessment of carbon exchange than traditional intermittent sampling.  
849 By integrating crop and soil components and applying dynamic partitioning models, the study  
850 quantified both respiration and photosynthesis fluxes at fine temporal resolution. The results  
851 revealed a clear 'fertile island' effect under tree canopies, with higher respiration and  
852 photosynthetic activity, and highlighted the significant contribution of *F. albida* trees to annual  
853 carbon uptake.

854 The consistency between chamber- and eddy covariance-based estimates reinforces the  
855 robustness of the methodology. Overall, this work underscores the role of *F. albida*-based  
856 agroforestry systems ~~in the dynamic of C exchanges as effective carbon sinks~~ in semi-arid  
857 environments, offering valuable insights for carbon accounting and sustainable land management  
858 in the Sahel.

a mis en forme : Police :Italique

859 **Acknowledgments**

860 This research was financially supported by the CaSSECS project (Carbon Sequestration and  
861 Greenhouse Gas Emissions in (Agro) Silvopastoral Systems of the CILS-Sahel States  
862 (FOOD/2019/410-169), within the framework of the European Union's initiative 'Development  
863 of Smart Innovation through Agricultural Research' (DeSIRA-UE-EuropAID). We extend our  
864 sincere gratitude to the coordination team of the CaSSECS project, the "Laboratoire Mixte  
865 International Intensification Écologique des Sols Cultivés en Afrique de l'Ouest" (LMI IESOL) of  
866 the of the French National Institute for Development (IRD) in Dakar (Senegal), as well as to the  
867 Faidherbia-Flux platform (<https://lped.info/wikiObsSN/?Faidherbia-Flux>), its partners, and  
868 affiliated projects: [EU-H2020 \[SUSTAIN-SAHEL \(Grant N° 861974\)\]](#); [ANR under the](#)  
869 [France 2030 program \[PEPR FairCarboN-RIFT \(reference ANR-22-PEXF-0004\)\]](#); [EU-](#)  
870 [HORIZON EUROPE \[GALILEO \(Grant N° 101181623\) \]](#). ~~[PEPR FairCarbonN/PC3-RIFT, EU-](#)~~  
871 ~~[H2020 \[SUSTAIN-SAHEL \(Grant N° 861974\)\] and EU HORIZON EUROPE \[GALILEO \(Grant N°](#)~~  
872 ~~[101181623\)\]](#)~~. Our deepest appreciation goes to Ibou Diouf, the observer at our experimental site.  
873 Tagesson also acknowledged funding from Formas (Dnr 2021-00644). [Lastly, we are deeply](#)  
874 [grateful to the two reviewers, Riccardo Picone and Jim Boonman, for their insightful and](#)  
875 [highly constructive comments.](#)

876 **Author contribution: CRediT**

877 **Seydina Mohamad BA:** Conducting in situ experiments, collecting and processing data,  
878 writing-original draft, review and editing. **Olivier Roupsard:** Designing experimental  
879 apparatus and methodology, writing, review and editing. **Lydie Chapuis-Lardy:** Designing  
880 methodology, writing, review and editing. **Yélognissè Agbohessou:** Processing data,  
881 review and editing. **Fred Bouvery:** Designing chambers and connection to the instrument,  
882 review and editing. **Maxime Duthoit:** Designing experimental set and methodology,  
883 review and editing. **Aleksander Wieckowski:** Review and editing. **Mohamed Habibou**  
884 **Assouma:** Review and editing. **Espoir Gaglo:** Processing data, review and editing. **Claire**  
885 **Delon:** review and editing. **Torbern Tagesson:** Designing methodology, review, and  
886 editing. **Bienvenu Sambou:** Review and editing. **Dominique Serça:** Designing methodology,  
887 writing, review and editing.

888 **References**

- 889 Agbohessou, Y., Delon, C., Mougin, E., Grippa, M., Tagesson, T., Diedhiou, M., Ba, S., Ngom, D., Vezy,  
890 R., Ndiaye, O., Assouma, M. H., Diawara, M., & Roupsard, O.: To what extent are greenhouse-gas  
891 emissions offset by trees in a Sahelian silvopastoral system?, *Agr. Forest. Meteorol.*, 343, 109780,  
892 <https://doi.org/10.1016/j.agrformet.2023.109780>, 2023.
- 893 Agbohessou, Y., Delon, C., Grippa, M., Mougin, E., Ngom, D., Gaglo, E. K., Ndiaye, O., Salgado, P., and  
894 Roupsard, O.: Modelling CO<sub>2</sub> and N<sub>2</sub>O emissions from soils in silvopastoral systems of the West  
895 African Sahelian band. *Biogeosciences*, 21, 2811–2837, [https://doi.org/10.5194/bg-21-2811-](https://doi.org/10.5194/bg-21-2811-2024)  
896 [2024](https://doi.org/10.5194/bg-21-2811-2024), 2024.
- 897 Ago, E., Agbossou, K., Ozer, P., & Aubinet, M.: Mesure des flux de CO<sub>2</sub> et séquestration de carbone  
898 dans les écosystèmes terrestres ouest-africains (synthèse bibliographique), *Biotechnologie*,  
899 *Biotechnol. Agron. Soc. Environ.*, 20(1), 68-82, <https://doi.org/10.25518/1780-4507.12565>,  
900 2016a.
- 901 Ago, E., Agbossou, E. K., Cohard, J. M., Galle, S., & Aubinet, M.: Response of CO<sub>2</sub> fluxes and  
902 productivity to water availability in two contrasting ecosystems in northern Benin (West Africa),  
903 *Ann. Forest. Sci.*, 73(2), 483-500, <https://doi.org/10.1007/s13595-016-0542-9>, 2016b.
- 904 Ago, E., Agbossou, E. K., Galle, S., Cohard, J. M., Heinesch, B., & Aubinet, M.: Long term observations  
905 of carbon dioxide exchange over cultivated savanna under a Sudanian climate in Benin (West  
906 Africa), *Agr. Forest. Meteorol.*, 197, 13-25, <https://doi.org/10.1016/j.agrformet.2014.06.005>,  
907 2014.
- 908 Archibald, S. A., Kirton, A., van der Merwe, M.R, Scholes, R. J., Williams, C.A, & Hanan, H.: Drivers of  
909 inter-annual variability in Net Ecosystem Exchange in a semi-arid savanna ecosystem, South  
910 Africa, *Biogeosciences*, 6, 251–266, <https://doi.org/10.5194/bg-6-251-2009>, 2009.
- 911 Ardö, J., Mölder, M., El-Tahir, B. A., & Elkhidir, H. A. M.: Seasonal variation of carbon fluxes in a  
912 sparse savanna in semi-arid Sudan, *Carbon Balance and Management*, 3(1), 7,  
913 <https://doi.org/10.1186/1750-0680-3-7>, 2008.
- 914 Assefa, A., Muthuri, C. W., Gebrekirstos, A., Hadgu, K., & Fetene, M.: Tree growth and wheat  
915 productivity are affected by pollarding *Faidherbia albida* in semi-arid Ethiopia, *Agroforest. Syst.*,  
916 98(3), 783-796, <https://doi.org/10.1007/s10457-023-00948-7>, 2024.

Code de champ modifié

917 Assouma, M. H., Hiernaux, P., Lecomte, P., Ickowicz, A., Bernoux, M., & Vayssières, J.: Contrasted  
918 seasonal balances in a Sahelian pastoral ecosystem result in a neutral annual carbon balance,  
919 *Journal of Arid Environments*, 162, 62-73, <https://doi.org/10.1016/j.jaridenv.2018.11.013>, 2019.

920 Assouma, M. H., Serça, D., Guérin, F., Blanfort, V., Lecomte, P., Touré, I., Ickowicz, A., Manlay, R. J.,  
921 Bernoux, M., & Vayssières, J.: Livestock induces strong spatial heterogeneity of soil CO<sub>2</sub>, N<sub>2</sub>O and  
922 CH<sub>4</sub> emissions within a semi-arid sylvo-pastoral landscape in West Africa, *Journal of Arid Land*,  
923 9(2), 210-221, <https://doi.org/10.1007/s40333-017-0001-y>, 2017.

924 Bado, B. V., Whitbread, A., & Sanoussi Manzo, M. L.: Improving agricultural productivity using  
925 agroforestry systems: Performance of millet, cowpea, and ziziphus-based cropping systems in  
926 West Africa Sahel, *Agr. Ecosyst. Environ.*, 305, 107175,  
927 <https://doi.org/10.1016/j.agee.2020.107175>, 2021.

928 Bahn, M., Reichstein, M., Davidson, E. A., Grünzweig, J., Jung, M., Carbone, M. S., Epron, D., Misson,  
929 L., Nouvellon, Y., Rouspard, O., Savage, K., Trumbore, S. E., Gimeno, C., Curiel Yuste, J., Tang, J.,  
930 Vargas, R., & Janssens, I. A.: Soil respiration at mean annual temperature predicts annual total  
931 across vegetation types and biomes, *Biogeosciences*, 7(7), 2147-2157,  
932 <https://doi.org/10.5194/bg-7-2147-2010>, 2010.

933 Baldocchi, D.: Assessing the eddy covariance technique for evaluating carbon dioxide exchange  
934 rates of ecosystems: Past, present and future, *Glob. Change Biol.*, 9, 479-492,  
935 <https://doi.org/10.1046/j.1365-2486.2003.00629.x>, 2003.

936 Baldocchi, D.: « Breathing » of the terrestrial biosphere: Lessons learned from a global network of  
937 carbon dioxide flux measurement systems, *Aust. J. Bot.*, 56(1), 1,  
938 <https://doi.org/10.1071/BT07151>, 2008.

939 Baldocchi, D.: How eddy covariance flux measurements have contributed to our understanding of  
940 global change biology, *Glob. Change Biol.*, 26: 242-260, <https://doi.org/10.1111/gcb.14807>,  
941 2020.

942 Barnard, R. L., Blazewicz, S. J., & Firestone, M. K.: Rewetting of soil: Revisiting the origin of soil CO<sub>2</sub>  
943 emissions, *Soil Biology and Biochemistry*, 147, <https://doi.org/10.1016/j.soilbio.2020.107819>,  
944 2020.

945 Bastviken, D., Wilk, J., Duc, N. T., Gålfalk, M., Karlson, M., Neset, T.-S., Opach, T., Enrich-Prast, A., &  
946 Sundgren, I.: Critical method needs in measuring greenhouse gas fluxes. *Environmental Research*  
947 *Letters*, 17(10), 104009, <https://doi.org/10.1088/1748-9326/ac8fa9>, 2022.

948 Bayala, J., Sanou, J., Bazié, H. R., Coe, R., Kalinganire, A., & Sinclair, F. L.: Regenerated trees in  
949 farmers' fields increase soil carbon across the Sahel, *Agroforest. Syst.*, 94(2), 401-415,  
950 <https://doi.org/10.1007/s10457-019-00403-6>, 2020.

951 Birch, H. F.: The effect of soil drying on humus decomposition and nitrogen availability, *Plant and*  
952 *Soil*, 10(1), 9-31, <https://doi.org/10.1007/BF01343734>, 1958.

953 Bombelli A, Henry M, Castaldi S, Adu-Bredu S, Arneth A, De Grandcourt A, Grieco E., Kutsch  
954 W.L., Lehsten V., Rasile A., Reichstein M, Tansey K., Weber U, Valentini R.: An outlook on the Sub-  
955 Saharan Africa carbon balance, *Biogeosciences*, 6 (10), 2193-2205, [https://doi.org/10.5194/bg-](https://doi.org/10.5194/bg-6-2193-2009)  
956 [6-2193-2009](https://doi.org/10.5194/bg-6-2193-2009), 2009.

957 Boriken, W., Xu, Y., Davidson, E. A., & Beese, F.: Site and temporal variation of soil respiration in  
958 European beech, Norway spruce, and Scots pine forests, *Glob. Change Biol.*, 8(12), 1205-1216,  
959 <https://doi.org/10.1046/j.1365-2486.2002.00547.x>, 2002.

960 Bréchet, L. M., Daniel, W., Stahl, C., Burban, B., Goret, J. Y., Salomón, R. L., & Janssens, I. A.:  
961 Simultaneous tree stem and soil greenhouse gas (CO<sub>2</sub>, CH<sub>4</sub>, N<sub>2</sub>O) flux measurements: A novel  
962 design for continuous monitoring towards improving flux estimates and temporal resolution, *New*  
963 *Phytologist*, 230(6), 2487-2500, <https://doi.org/10.1111/nph.17352>, 2021.

964 Bréchet, L. M., Salomón, R. L., Machacova, K., Stahl, C., Burban, B., Goret, J. Y., Steppe, K., Damien, B.,  
965 & Janssens, I. A.: Insights into the sub daily variations in methane, nitrous oxide and carbon  
966 dioxide fluxes from upland tropical tree stems, *New Phytologist*, 20401,  
967 <https://doi.org/10.1111/nph.20401>, 2025.

968 Brümmer, C., Falk, U., Papen, H., Szarzynski, J., Wassmann, R., & Brüggemann, N.: Diurnal, seasonal,  
969 and interannual variation in carbon dioxide and energy exchange in shrub savanna in Burkina  
970 Faso (West Africa), *Biogeosciences*, 113, G2030, <https://doi.org/10.1029/2007JG000583>, 2008.

971 Brümmer, C., Papen, H., Wassmann, R., & Brüggemann, N.: Fluxes of CH<sub>4</sub> and CO<sub>2</sub> from soil and  
972 termite mounds in south Sudanian savanna of Burkina Faso (West Africa), *Global Biogeochemical*  
973 *Cycles*, 23, GB1001, <https://doi.org/10.1029/2008GB003237>, 2009.

974 Cardinael, R., Cadisch, G., Gosme, M., Oelbermann, M., & Van Noordwijk, M.: Climate change  
975 mitigation and adaptation in agriculture: Why agroforestry should be part of the solution? *Agr.*  
976 *Ecosyst. Environ.*, 319, 107555, <https://doi.org/10.1016/j.agee.2021.107555>, 2021.

977 Charbonnier, F., Roupsard, O., le Maire, G., Guillemot, J., Casanoves, F., Lacoïnte, A., Vaast, P.,  
978 Allinne, C., Audebert, L., Cambou, A., Clément-Vidal, A., Defrenet, E., Duursma, R. A., Jarri, L.,  
979 Jourdan, C., Khac, E., Leandro, P., Medlyn, B. E., Saint-André, L., Thaler, P., Van Den Meersche, K.,  
980 Barquero Aguilar, A., Lehner, P., & Dreyer, E.: Increased light-use efficiency sustains net primary  
981 productivity of shaded coffee plants in agroforestry system, *Plant Cell and Environment*, 40(8),  
982 1592-1608, <https://doi.org/10.1111/pce.12964>, 2017.

983 Chu, H., Luo, X., Ouyang, Z., et al.: Representativeness of Eddy-Covariance flux footprints for areas  
984 surrounding AmeriFlux sites, *Agr. Forest. Meteorol.*, 301-302, 108350,  
985 <https://doi.org/10.1016/j.agrformet.2021.108350>, 2021.

986 Clermont-Dauphin, C., N'dienor, M., Leroux, L., Ba, Halimatou. S., Bongers, F., Jourdan, C., Roupsard,  
987 O., Do, F. C., Cournac, L., & Seghieri, J.: Faidherbia albida trees form a natural buffer against millet  
988 water stress in agroforestry parklands in Senegal, *Biotechnol. Agron. Soc. Environ.*, 182-195,  
989 <https://doi.org/10.25518/1780-4507.20477>, 2023.

990 Conant, R. T., Dalla-Betta, P., Klopatek, C. C., & Klopatek, J. M.: Controls on soil respiration in  
991 semiarid soils, *Soil Biology and Biochemistry*, 36(6), 945-951,  
992 <https://doi.org/10.1016/j.soilbio.2004.02.013>, 2004.

993 Crosson, E.: A cavity ring-down analyzer for measuring atmospheric levels of methane, carbon  
994 dioxide, and water vapor, *App. Phys. B-Lasers O.*, 92, 403-408, [https://doi.org/10.1007/s00340-](https://doi.org/10.1007/s00340-008-3135-y)  
995 [008-3135-y](https://doi.org/10.1007/s00340-008-3135-y), 2008.

996 de Carvalho, A. F., Fernandes-Filho, E. I., Daher, M., Gomes, L. de C., Cardoso, I. M., Fernandes, R. B.  
997 A., & Schaefer, C. E. G. R.: Microclimate and soil and water loss in shaded and unshaded  
998 agroforestry coffee systems, *Agroforest. Syst.*, 95(1), 119-134, [https://doi.org/10.1007/s10457-](https://doi.org/10.1007/s10457-020-00567-6)  
999 [020-00567-6](https://doi.org/10.1007/s10457-020-00567-6), 2021.

1000 Delon, C., Galy-Lacaux, C., Serça, D., Personne, E., Mougin, E., Adon, M., ... & Tagesson, T.: Modelling  
1001 land-atmosphere daily exchanges of NO, NH<sub>3</sub>, and CO<sub>2</sub> in a semi-arid grazed ecosystem in Senegal,  
1002 *Biogeosciences*, 16(9), 2049-2077, <https://doi.org/10.5194/bg-16-2049-2019>, 2019.

1003 Delaunay, V., Desclaux, A., & Sokhna, Ch.: Niakhar, mémoires et perspectives : Recherches  
1004 pluridisciplinaires sur le changement en Afrique, IRD Éditions/L'Harmattan, 536 p., ISBN  
1005 9782140103551, 2140103556 [https://www.editions.ird.fr/open\\_access\\_download/851/441](https://www.editions.ird.fr/open_access_download/851/441),  
1006 2019.

Code de champ modifié

Code de champ modifié

1007 DeLucia, E. H., Drake, J. E., Thomas, R. B., & Gonzalez-Meler, M.: Forest carbon use efficiency: Is  
1008 respiration a constant fraction of gross primary production?, *Glob. Change Biol.*, 13(6),  
1009 1157-1167, <https://doi.org/10.1111/j.1365-2486.2007.01365.x>, 2007.

1010 Denmead, O. T.: Approaches to measuring fluxes of methane and nitrous oxide between  
1011 landscapes and the atmosphere, *Plant and Soil*, 309(1-2), 5-24, [https://doi.org/10.1007/s11104-](https://doi.org/10.1007/s11104-008-9599-z)  
1012 [008-9599-z](https://doi.org/10.1007/s11104-008-9599-z), 2008.

1013 Diack, I., Diene, S., Leroux, L., Diouf, A., Benjamin, H., Olivier, R., Letourmy, P., Alain, A., Sarr, I., &  
1014 Moussa, D.: Combining UAV and Sentinel-2 Imagery for Estimating Millet FCover in a  
1015 Heterogeneous Agricultural Landscape of Senegal, *IEEE Journal of Selected Topics in Applied*  
1016 *Earth Observations and Remote Sensing*, 17, 7305-7322,  
1017 <https://doi.org/10.1109/ISTARS.2024.3373508>, 2024.

1018 Diene, S. M., Diack, I., Audebert, A., Roupsard, O., Leroux, L., Diouf, A. A., Mbaye, M., Fernandez, R.,  
1019 Diallo, M., Sarr, I.: Improving pearl millet yield estimation from UAV imagery in the semiarid  
1020 agroforestry system of Senegal through textural indices and reflectance normalization, in *IEEE*  
1021 *Access*, 12, 132626-132643, <https://doi.org/10.1109/ACCESS.2024.3460107>, 2024.

1022 Dilla, A. M., Smethurst, P. J., Barry, K., & Parsons, D.: Preliminary estimate of carbon sequestration  
1023 potential of *Faidherbia albida* (Delile) A. Chev in an agroforestry parkland in the Central Rift Valley  
1024 of Ethiopia, *Forests, Trees and Livelihoods*, 28(2), 79-89,  
1025 <https://doi.org/10.1080/14728028.2018.1564146>, 2019.

1026 Diongue, D., Brunetti, G., Stumpp, C., Do, F., Roupsard, O., Orange, D., Faye, W., Sow, S., Jourdan, C.,  
1027 & Faye, S.: A Probabilistic Framework for Assessing the Hydrological Impact of *Faidherbia Albida*  
1028 in an Arid Area of Senegal, *Journal of Hydrology*, 622, 129717,  
1029 <https://doi.org/10.1016/j.jhydrol.2023.129717>, 2023.

1030 Diongue, D. M. L., Roupsard, O., Do, F. C., Stumpp, C., Orange, D., Sow, S., Jourdan, C., & Faye, S.:  
1031 Evaluation of parameterisation approaches for estimating soil hydraulic parameters with  
1032 HYDRUS-1D in the groundnut basin of Senegal, *Hydrological Sciences Journal*, 67(15), 2327-  
1033 2343, <https://doi.org/10.1080/02626667.2022.2142474>, 2022.

1034 Duthoit, M., Roupsard, O., Créquy, N., & Sauze, J.: Conception d'un dispositif automatisé de  
1035 chambres de mesures d'échanges gazeux du sol à fermeture horizontale, *Le Cahier des Techniques*  
1036 de l'Inra, 102, 19 p., hal-03989886, <https://hal.science/hal-03989886/document>, 2020.

Code de champ modifié

1037 Eldridge, D.J., Ding, J., Dorrough, J. et al. Hotspots of biogeochemical activity linked to aridity and  
1038 plant traits across global drylands. *Nat. Plants* 10, 760–770 (2024).  
1039 <https://doi.org/10.1038/s41477-024-01670-7>

1040 Evans, S., Dieckmann, U., Franklin, O., & Kaiser, C.: Synergistic effects of diffusion and microbial  
1041 physiology reproduce the Birch effect in a micro-scale model, *Soil Biology and Biochemistry*, 93,  
1042 28-37, <https://doi.org/10.1016/j.soilbio.2015.10.020>, 2016.

1043 Falge, E., Baldocchi, D., Olson, R., Anthoni, P., Aubinet, M., Bernhofer, C., Burba, G., Ceulemans, R.,  
1044 Clement, R., Dolman, H., Granier, A., Gross, P., Grünwald, T., Hollinger, D., Jensen, N.-O., Katul, G.,  
1045 Keronen, P., Kowalski, A., Ta Lai, C., ... Oren, R.: Gap filling strategies for defensible annual sums of  
1046 net ecosystem exchange, *Agr. Forest Meteorol.*, 107, 43-69, [https://doi.org/10.1016/S0168-1923\(00\)00225-2](https://doi.org/10.1016/S0168-1923(00)00225-2), 2001.

1048 Fan, Z., Neff, J. C., & Hanan, N. P.: Modeling pulsed soil respiration in an African savanna ecosystem,  
1049 *Agr. Forest Meteorol.*, 200, 282-292, <https://doi.org/10.1016/j.agrformet.2014.10.009>, 2015.

1050 Fang, F., Han, X., Liu, W., & Tang, M.: Carbon dioxide fluxes in a farmland ecosystem of the southern  
1051 Chinese Loess Plateau measured using a chamber-based method, *PeerJ*, 8, 8994,  
1052 <https://doi.org/10.7717/peerj.8994>, 2020.

1053 Faye, W., Fall, A. N., Orange, D., Do, F., Roupsard, O., & Kane, A.: Climatic variability in the Sine-  
1054 Saloum basin and its impacts on water resources: Case of the Sob and Diohine watersheds in the  
1055 region of Niakhar, *Proceedings of the International Association of Hydrological Sciences*, 383,  
1056 391-399, <https://doi.org/10.5194/piahs-383-391-2020>, 2020.

1057 Finkelstein, P. L., & Sims, P. F.: Sampling error in eddy correlation flux measurements, *J. Geophys.*  
1058 *Res.*, 106(D4), 3503–3509, <https://doi.org/10.1029/2000JD900731>, 2001.

1059 Fleck, D., He, Y., Alexander, C., Jacobson, G., & Cunningham, K. L.: Simultaneous soil flux  
1060 measurements of five gases-N<sub>2</sub>O, CH<sub>4</sub>, CO<sub>2</sub>, NH<sub>3</sub>, and H<sub>2</sub>O-with the Picarro G2508," Picarro  
1061 Application Note, AN034,  
1062 [https://www.picarro.com/sites/default/files/product\\_documents/Picarro\\_AN034\\_Soil%20Flux%20with%20the%20G2508\\_1.pdf](https://www.picarro.com/sites/default/files/product_documents/Picarro_AN034_Soil%20Flux%20with%20the%20G2508_1.pdf), 2013.

1064 Foken, T., Göockede, M., Mauder, M., Mahrt, L., Amiro, B., Munger, W.: Post-Field Data Quality  
1065 Control, In: Lee, X., Massman, W., Law, B. (eds) *Handbook of Micrometeorology*, *Atmos. Ocean. Sci.*  
1066 *Lib.*, vol 29, Springer, Dordrecht, [https://doi.org/10.1007/1-4020-2265-4\\_9](https://doi.org/10.1007/1-4020-2265-4_9), 2004.

1067 Foken, T., Aubinet, M., & Leuning, R.: Eddy Covariance. In M. Aubinet, T. Vesala, & D. Papale (eds),  
1068 Eddy Covariance, p.1-19, Springer, Netherlands, <https://doi.org/10.1007/978-94-007-2351-1>,  
1069 2012.

1070 Fox, J., Weisberg, S., & Price, B.: car: Companion to Applied Regression (version 3.1-3) [Dataset].  
1071 <https://doi.org/10.32614/CRAN.package.car>, 2023.

1072 Gomes, L. D. C., Cardoso, I. M., Mendonça, E. D. S., Fernandes, R. B. A., Lopes, V. S., & Oliveira, T. S.:  
1073 Trees modify the dynamics of soil CO<sub>2</sub> efflux in coffee agroforestry systems, *Agr. Forest. Meteorol.*,  
1074 224, 30-39, <https://doi.org/10.1016/j.agrformet.2016.05.001>, 2016.

1075 Gonsamo, A., Chen, J. M., He, L., Sun, Y., Rogers, C., & Liu, J.: Exploring SMAP and OCO-2 observations  
1076 to monitor soil moisture control on photosynthetic activity of global drylands and croplands,  
1077 *Remote Sensing of Environment*, 232, 111314, <https://doi.org/10.1016/j.rse.2019.111314>, 2019.

1078 Guillen-Cruz, G., Campuzano, E. F., Juárez-Altamirano, R., López-García, K. L., Torres-Arreola, R., &  
1079 Flores-Rentería, D.: Interannual Variation and Control Factors of Soil Respiration in Xeric  
1080 Shrubland and Agricultural Sites from the Chihuahuan Desert, Mexico, *Land*, 12(11), 1961,  
1081 <https://doi.org/10.3390/land12111961>, 2023.

1082 Gupta, S.R., Dagar, J.C., Sileshi, G.W., Chaturvedi, R.K.: Agroforestry for Climate Change Resilience  
1083 in Degraded Landscapes. In: Dagar, J.C., Gupta, S.R., Sileshi, G.W. (eds) *Agroforestry for Sustainable*  
1084 *Intensification of Agriculture in Asia and Africa*, Sustainability Sciences in Asia and Africa,  
1085 Springer, Singapore. [https://doi.org/10.1007/978-981-19-4602-8\\_5](https://doi.org/10.1007/978-981-19-4602-8_5), 2023.

1086 Houghton, R. A. and Hackler, J. L.: Emissions of carbon from land use change in sub-Saharan Africa,  
1087 *Geophys. Res.*, 111, G02003, <https://doi.org/10.1029/2005JG000076>, 2006.

1088 IUSS Working Group WRB.: World Reference Base for Soil Resources. International soil  
1089 classification system for naming soils and creating legends for soil maps, 4th edition, International  
1090 Union of Soil Sciences (IUSS), Vienna, Austria, ISBN 979-8-9862451-1-9,  
1091 [www.isric.org/sites/default/files/WRB\\_fourth\\_edition\\_2022-12-18.pdf](http://www.isric.org/sites/default/files/WRB_fourth_edition_2022-12-18.pdf), 2022.

1092 Jackson, R.B., Canadell, J., Ehleringer, J.R. et al.: A global analysis of root distributions for terrestrial  
1093 biomes, *Oecologia* 108, 389–411, <https://doi.org/10.1007/BF00333714>, 1996.

1094 Jevon, F. V., Gewirtzman, J., Lang, A. K., Ayres, M. P., & Matthes, J. H.: Tree Species Effects on Soil  
1095 CO<sub>2</sub> and CH<sub>4</sub> Fluxes in a Mixed Temperate Forest, *Ecosystems*, 26(7), 1587-1602,  
1096 <https://doi.org/10.1007/s10021-023-00852-2>, 2023.

1097 Jia, X., Mu, Y., Zha, T., Wang, B., Qin, S., & Tian, Y.: Seasonal and interannual variations in ecosystem  
1098 respiration in relation to temperature, moisture, and productivity in a temperate semi-arid  
1099 shrubland, *Science of The Total Environment*, 709, 136210,  
1100 <https://doi.org/10.1016/j.scitotenv.2019.136210>, 2020.

1101 [Juszczak, R., Acosta, M., Olejnik, J.: Comparison of Daytime and Nighttime Ecosystem Respiration](#)  
1102 [Measured by the Closed Chamber Technique on a Temperate Mire in Poland, \*Pol. J. Environ. Stud.\*](#)  
1103 [Vol. 21, No. 3, 643-658, 2012.](#)

1104 Kim, D. G., Vargas, R., Bond-Lamberty, B., & Turetsky, M. R.: Effects of soil rewetting and thawing  
1105 on soil gas fluxes: A review of current literature and suggestions for future research,  
1106 *Biogeosciences*, 9(7), 2459-2483, <https://doi.org/10.5194/bg-9-2459-2012>, 2012.

1107 Kim, D.-G., Thomas, A. D., Pelster, D., Rosenstock, T. S., & Sanz-Cobena, A.: Greenhouse gas  
1108 emissions from natural ecosystems and agricultural lands in sub-Saharan Africa: Synthesis of  
1109 available data and suggestions for further research, *Biogeosciences*, 13(16), 4789-4809,  
1110 <https://doi.org/10.5194/bg-13-4789-2016>, 2016.

1111 Klaus, M., Öquist, M., & Macháčová, K.: Tree stem-atmosphere greenhouse gas fluxes in a boreal  
1112 riparian forest, *Science of The Total Environment*, 954, 176243,  
1113 <https://doi.org/10.1016/j.scitotenv.2024.176243>, 2024.

1114 Kormann, R., & Meixner, F. X.: An analytical footprint model for non-neutral stratification,  
1115 *Boundary-Layer Meteorology*, 99, 207-224, <https://doi.org/10.1023/A:1018991015119>, 2001.

1116 Kuyah, S., Whitney, C. W., Jonsson, M., Sileshi, G. W., Öborn, I., Muthuri, C. W., & Luedeling, E.:  
1117 Agroforestry delivers a win-win solution for ecosystem services in sub-Saharan Africa. A meta-  
1118 analysis, *Agronomy for Sustainable Development*, 39(5), [https://doi.org/10.1007/s13593-019-](https://doi.org/10.1007/s13593-019-0589-8)  
1119 [0589-8](https://doi.org/10.1007/s13593-019-0589-8), 2019.

1120 Lambers, H., Chapin, F. S., & Pons, T. L.: *Plant Physiological Ecology*, Springer New York.  
1121 <https://doi.org/10.1007/978-0-387-78341-3>, 2008.

1122 Lasslop, G., Reichstein, M., Papale, D., Richardson, A., Arneth, A., Barr, A., Stoy, P., & Wohlfahrt, G.:  
1123 Separation of net ecosystem exchange into assimilation and respiration using a light response  
1124 curve approach: Critical issues and global evaluation, *Glob. Change Biol.*, 16(1), 187-208.  
1125 <https://doi.org/10.1111/j.1365-2486.2009.02041.x>, 2010.

- 1126 Lembrechts J.J., Aalto J, Ashcroft MB, et al.: SoilTemp: A global database of near-surface  
1127 temperature, *Glob. Change Biol.*, 26, 6616–6629, <https://doi.org/10.1111/gcb.15123>, 2020.
- 1128 Lembrechts, J. J., van den Hoogen, J., Aalto, J., et al.: Global maps of soil temperature. *Glob. Change*  
1129 *Biol.*, 28, 3110-3144, <https://doi.org/10.1111/gcb.16060>, 2022.
- 1130 Leroux, L., Falconnier, G. N., Diouf, A. A., Ndao, B., Gbodjo, J. E., Tall, L., Balde, A. A., Clermont-  
1131 Dauphin, C., Bégué, A., Affholder, F., & Roupsard, O.: Using remote sensing to assess the effect of  
1132 trees on millet yield in complex parklands of Central Senegal, *Agr. Syst.*, 184,  
1133 <https://doi.org/10.1016/j.agsy.2020.102918>, 2020.
- 1134 Liu, W., Zhang, Z., & Wan, S.: Predominant role of water in regulating soil and microbial respiration  
1135 and their responses to climate change in a semiarid grassland, *Glob. Change Biol.*, 15(1), 184-195,  
1136 <https://doi.org/10.1111/j.1365-2486.2008.01728.x>, 2009.
- 1137 Liu, Y., He, N., Wen, X., Xu, L., Sun, X., Yu, G., Liang, L., & Schipper, L. A.: The optimum temperature  
1138 of soil microbial respiration: Patterns and controls, *Soil Biology and Biochemistry*, 121, 35-42,  
1139 <https://doi.org/10.1016/j.soilbio.2018.02.019>, 2018.
- 1140 Lloyd, J., & Taylor, J. A.: On the Temperature Dependence of Soil Respiration, *Functional Ecology*,  
1141 8(3), 315-323, <https://doi.org/10.2307/2389824>, 1994.
- 1142 Lopes, V. S., Cardoso, I. M., Cavalcante, V. S., Gomes, L. de C., Tanure, M. M. C., Moura, W. de M.,  
1143 Mendonça, E. de S., & Fernandes, R. B. A.: Soil CO<sub>2</sub> efflux in coffee agroforestry and full-sun coffee  
1144 systems, *Acta Sci. – Agr*, 46(1), e65877, <https://doi.org/10.4025/actasciagron.v46i1.65877>,  
1145 2024.
- 1146 Lüdecke, D., Ben-Shachar, M., Patil, I., Waggoner, P., & Makowski, D.: Performance: An R Package  
1147 for Assessment, Comparison and Testing of Statistical Models, *Journal of Open-Source Software*,  
1148 6(60), 3139, <https://doi.org/10.21105/joss.03139>, 2021.
- 1149 Luo, Y., & Zhou, X.: Methods of Measurements and Estimations. In Y. Luo & X. Zhou (eds) *Soil*  
1150 *Respiration and Environment*, 161-185 p., Academic Press, Elsevier,  
1151 <https://doi.org/10.1016/B978-0-12-088782-8.X5000-1>, 2006.
- 1152 Macharia, J. M., Pelster, D. E., Ngetich, F. K., Shisanya, C. A., Mucheru-Muna, M., & Mugendi, D. N.:  
1153 Soil greenhouse gas fluxes from maize production under different soil fertility management  
1154 practices in East Africa, *Journal of Geophysical Research: Biogeosciences*, 125(7),  
1155 e2019JG005427, <https://doi.org/10.1029/2019JG005427>, 2020.

1156 Malou, O. P., Moulin, P., Chevallier, T., Masse, D., Vayssières, J., Badiane-Ndour, N. Y., Tall, L., Thiam,  
1157 A., & Chapuis-Lardy, L.: Estimates of carbon stocks in sandy soils cultivated under local  
1158 management practices in Senegal's groundnut basin, *Regional Environmental Change*, 21(3), 65,  
1159 <https://doi.org/10.1007/s10113-021-01790-2>, 2021.

1160 Manzoni, S., Chakrawal, A., Fischer, T., Schimel, J. P., Porporato, A., & Vico, G.: Rainfall  
1161 intensification increases the contribution of rewetting pulses to soil heterotrophic respiration,  
1162 *Biogeosciences*, 17(15), 4007-4023, <https://doi.org/10.5194/bg-17-4007-2020>, 2020.

1163 Mapanda, F., Mupini, J., Wuta, M., Nyamangara, J., & Rees, R. M.: A cross-ecosystem assessment of  
1164 the effects of land cover and land use on soil emission of selected greenhouse gases and related  
1165 soil properties in Zimbabwe, *European Journal of Soil Science*, 61(5), 721-733,  
1166 <https://doi.org/10.1111/j.1365-2389.2010.01266.x>, 2010.

1167 Mazza, G., Agnelli, A. E., & Lagomarsino, A.: The effect of tree species composition on soil C and N  
1168 pools and greenhouse gas fluxes in a Mediterranean reforestation, *Journal of Soil Science and Plant  
1169 Nutrition*, 21(2), 1339-1352, <https://doi.org/10.1007/s42729-021-00444-w>, 2021.

1170 Mbow, C., Van Noordwijk, M., Luedeling, E., Neufeldt, H., Minang, P. A., & Kowero, G.: Agroforestry  
1171 solutions to address food security and climate change challenges in Africa, *Current Opinion in  
1172 Environmental Sustainability*, 6(1), 61-67, <https://doi.org/10.1016/j.cosust.2013.10.014>, 2014.

1173 Meena, A., Hanief, M., Dinakaran, J., & Rao, K. S.: Soil moisture controls the spatio-temporal pattern  
1174 of soil respiration under different land use systems in a semi-arid ecosystem of Delhi, India,  
1175 *Ecological Processes*, 9(1), 15, <https://doi.org/10.1186/s13717-020-0218-0>, 2020.

1176 Meisner, A., Rousk, J., & Bååth, E.: Prolonged drought changes the bacterial growth response to  
1177 rewetting, *Soil Biology and Biochemistry*, 88, 314-322,  
1178 <https://doi.org/10.1016/j.soilbio.2015.06.002>, 2015.

1179 Merbold, L., Ardo, J., Arneth, A., Scholes, R. J., Nouvellon, Y., de Grandcourt, A., Archibald, S.,  
1180 Bonnefond, J. M., Boulain, N., Brueggemann, N., Bruemmer, C., Cappelaere, B., Ceschia, E., El-Khidir,  
1181 H. A. M., El-Tahir, B. A., Falk, U., Lloyd, J., Kergoat, L., Le Dantec, V. L., Mougou, E., Muchinda, M.,  
1182 Mukelabai, M. M., Ramier, D., Rouspard, O., Timouk, F., Veenendaal, E. M., & Kutsch, W. L.:  
1183 Precipitation as driver of carbon fluxes in 11 African ecosystems, *Biogeosciences*, 6:1027-1041,  
1184 <https://doi.org/10.5194/bg-6-1027-2009>, 2009.

1185 Moncrieff, J., Clement, R., Finnigan, J., Meyers, T.: Averaging, Detrending, and Filtering of Eddy  
1186 Covariance Time Series. In: Lee, X., Massman, W., Law, B. (eds) *Handbook of Micrometeorology*,

1187 Atmos. Ocean. Sci. Lib., vol 29, Springer, Dordrecht, [https://doi.org/10.1007/1-4020-2265-4\\_2](https://doi.org/10.1007/1-4020-2265-4_2),  
1188 2004.

1189 Moncrieff, J. B., Massheder, J. M., De Bruin, H., Elbers, J., Friborg, T., Heusinkveld, B., Kabat, P., Scott,  
1190 S., Soegaard, H., Verhoef, A.: A system to measure surface fluxes of momentum, sensible heat, water  
1191 vapour and carbon dioxide, Journal of Hydrology, 188, 589-611, [https://doi.org/10.1016/S0022-  
1192 1694\(96\)03194-0](https://doi.org/10.1016/S0022-1694(96)03194-0), 1997.

1193 Mosongo, P. S., Pelster, D. E., Li, X., Gaudel, G., Wang, Y., Chen, S., Li, W., Mburu, D., & Hu, C.:  
1194 Greenhouse Gas Emissions Response to Fertilizer Application and Soil Moisture in Dry  
1195 Agricultural Uplands of Central Kenya, Atmosphere, 13(3), 463,  
1196 <https://doi.org/10.3390/atmos13030463>, 2022.

1197 Muggeo, V.M.R.: Estimating regression models with unknown break-points. Statist. Med., 22:  
1198 3055-3071, <https://doi.org/10.1002/sim.1545>, 2003.

1199 Munjonji, L., Ntuli Innocentia, H., Ayisi, K. K., Dlamini, P., Mabitsela, K. E., Lehutjo, C. M., &  
1200 Magnificent Zwane, P. S.: Seasonal dynamics of soil CO<sub>2</sub> emissions from different semi-arid land-  
1201 use systems, Acta. Agr. Scand., Section BSP, 74(1), 2312934,  
1202 <https://doi.org/10.1080/09064710.2024.2312934>, 2024.

1203 Nickerson, N. R.: Evaluating gas emission measurements using Minimum Detectable Flux (MDF),  
1204 Eosene White papers, [https://eosense.com/wp-content/uploads/2019/11/Eosense-white-  
1205 paper-Minimum-Detectable-Flux.pdf](https://eosense.com/wp-content/uploads/2019/11/Eosense-white-paper-Minimum-Detectable-Flux.pdf), 2016.

1206 Owusu-Prempeh, N., Amekudzi, L. K., & Kyereh, B.: Assessment of soil carbon dioxide efflux from  
1207 contrasting land uses in a semi-arid savannah ecosystem, northeastern Ghana (West Africa),  
1208 Scientific African, 26, e02420, <https://doi.org/10.1016/j.sciaf.2024.e02420>, 2024.

1209 Oyonarte, C., Rey, A., Raimundo, J., Miralles, I., & Escribano, P.: The use of soil respiration as an  
1210 ecological indicator in arid ecosystems of the SE of Spain: Spatial variability and controlling  
1211 factors, Ecological Indicators, 14(1), 40-49, <https://doi.org/10.1016/j.ecolind.2011.08.013>,  
1212 2012.

1213 Padfield, D., Matheso, G., & Windram, F.: Package 'Nls. Multstart: Robust Non-Linear Regression  
1214 using AIC Scores (R package version 2.0.0)', [DOI:10.32614/CRAN.package.nls.multstart,  
1215 https://cran.r-project.org/web/packages/nls.multstart/nls.multstart.pdf](https://cran.r-project.org/web/packages/nls.multstart/nls.multstart.pdf), 2025.

1216 Pelster, D., Rufino, M., Rosenstock, T., Mango, J., Saiz, G., Diaz-Pines, E., Baldi, G., & Butterbach-Bahl,  
1217 K., Smallholder farms in eastern African tropical highlands have low soil greenhouse gas fluxes,  
1218 Biogeosciences, 14(1), 187-202, <https://doi.org/10.5194/bg-14-187-2017>, 2017.

1219 Picarro Inc.: PICARRO G2508 CRDS Analyzer N<sub>2</sub>O + CH<sub>4</sub> + CO<sub>2</sub> + NH<sub>3</sub> + H<sub>2</sub>O in Air, [Datasheet],  
1220 [https://www.picarro.com/sites/default/files/product\\_documents/Picarro\\_G2508%20Analyzer](https://www.picarro.com/sites/default/files/product_documents/Picarro_G2508%20Analyzer%20Datasheet.pdf)  
1221 [%20Datasheet.pdf](https://www.picarro.com/sites/default/files/product_documents/Picarro_G2508%20Analyzer%20Datasheet.pdf), 2015.

1222 Placella, S. A., Brodie, E. L., & Firestone, M. K.: Rainfall-induced carbon dioxide pulses result from  
1223 sequential resuscitation of phylogenetically clustered microbial groups, Proceedings of the  
1224 National Academy of Sciences, 109(27), 10931-10936,  
1225 <https://doi.org/10.1073/pnas.1204306109>, 2012.

1226

1227 Pontauiller, J. Y., Hymus, G. J., & Drake, B. G.: Estimation of leaf area index using ground-based  
1228 remote sensed NDVI measurements: Validation and comparison with two indirect techniques,  
1229 Canadian Journal of Remote Sensing, 29(3), 381-387, <https://doi.org/10.5589/m03-009>, 2003.

1230 Poyda, A., Reinsch, T., Skinner, R. H., Kluß, C., Loges, R., & Taube, F.: Comparing chamber and eddy  
1231 covariance based net ecosystem CO<sub>2</sub> exchange of fen soils; Journal of Plant Nutrition and Soil  
1232 Science, 180(2), 252-266, <https://doi.org/10.1002/jpln.201600447>, 2017.

1233 Qiu, R., Han, G., Li, S., Tian, F., Ma, X., & Gong, W.: Soil moisture dominates the variation of gross  
1234 primary productivity during hot drought in drylands, Science of The Total Environment, 899,  
1235 165686, <https://doi.org/10.1016/j.scitotenv.2023.165686>, 2023.

1236 Quansah, E., Mauder, M., Balogun, A. A., Amekudzi, L. K., Hingerl, L., Bliedernicht, J., & Kunstmann,  
1237 H.: Carbon dioxide fluxes from contrasting ecosystems in the Sudanian Savanna in West Africa,  
1238 Carbon Balance and Management, 10(1), 1. <https://doi.org/10.1186/s13021-014-0011-4>, 2015.

1239 Rabbi, S. M. F., Warren, C., Swarbrick, B., Minasny, B., Mcbratney, A., & Young, I.: Microbial  
1240 decomposition of organic matter and wetting-drying promotes aggregation in artificial soil but  
1241 porosity increases only in wet-dry condition, Geoderma, 447, 116924,  
1242 <https://doi.org/10.1016/j.geoderma.2024.116924>, 2024.

1243 Rahimi, J., Ago, E. E., Ayantunde, A., Berger, S., Bogaert, J., Butterbach-Bahl, K., Cappelaere, B.,  
1244 Cohard, J.-M., Demarty, J., Diouf, A. A., Falk, U., Haas, E., Hiernaux, P., Kraus, D., Roupsard, O., Scheer,  
1245 C., Srivastava, A. K., Tagesson, T., & Grote, R.: Modeling gas exchange and biomass production in

1246 West African Sahelian and Sudanian ecological zones, *Geoscientific Model Development*, 14(6),  
1247 3789-3812, <https://doi.org/10.5194/gmd-14-3789-2021>, 2021.

1248 Raich, J. W., Lambers, H., & Oliver, D. J.: Respiration in Terrestrial Ecosystems, In D. M. Karl, & W.  
1249 H., Schlesinger (Eds.), *Treatise on Geochemistry* (2 ed., Vol. 10, pp. 613-649), Elsevier,  
1250 <https://doi.org/10.1016/B978-0-08-095975-7.00817-2>, 2014.

1251 Ramesh, T., Manjaiah, K. M., Tomar, J. M. S., & Ngachan, S. V.: Effect of multipurpose tree species on  
1252 soil fertility and CO<sub>2</sub> efflux under hilly ecosystems of Northeast India, *Agr. Syst.*, 87(6), 1377-1388,  
1253 <https://doi.org/10.1007/s10457-013-9645-6>, 2013.

1254 R. Core Team.: *R: A language and environment for statistical computing*, R Foundation for  
1255 Statistical Computing, Vienna, Austria, 2023.

1256 Reichle, D. E.: Energy flow in ecosystems., In D.E. Reichle (ed) *The Global Carbon Cycle and Climate*  
1257 *Change* (p. 119-156), Elsevier, <https://doi.org/10.1016/B978-0-12-820244-9.00008-1>, (2020).

1258 [Reichstein, M., et al.: Modeling temporal and large-scale spatial variability of soil respiration from](#)  
1259 [soil water availability, temperature and vegetation productivity indices. \*Global Biogeochem.\*](#)  
1260 [Cycles, 17, 1104. doi:10.1029/2003GB002035. 4, 2003.](#)

1261 Reichstein, M., Falge, E., Baldocchi, D., Papale, D., Aubinet, M., Berbigier, P., Bernhofer, C.,  
1262 Buchmann, N., Gilmanov, T., Granier, A., Grünwald, T., Havránková, K., Ilvesniemi, H., Janous, D.,  
1263 Knohl, A., Laurila, T., Lohila, A., Loustau, D., Matteucci, G., ... Valentini, R.: On the separation of net  
1264 ecosystem exchange into assimilation and ecosystem respiration: Review and improved  
1265 algorithm, *Glob. Change Biol.*, 11(9), 1424-1439, [https://doi.org/10.1111/j.1365-](https://doi.org/10.1111/j.1365-2486.2005.001002.x)  
1266 [2486.2005.001002.x](#), 2005.

1267 Reum, F., Gerbig, C., Lavric, J. V., Rella, C. W., & Göckede, M.: Correcting atmospheric CO<sub>2</sub> and CH<sub>4</sub>  
1268 mole fractions obtained with Picarro analyzers for sensitivity of cavity pressure to water vapor,  
1269 *Atmos. Meas. Tech.*, 12(2), 1013-1027, <https://doi.org/10.5194/amt-12-1013-2019>, 2005.

1270 Rheault, K., Riis Christiansen, J., & Steenberg Larsen, K.: The role of tree species and microbes for  
1271 the development of net greenhouse gas fluxes from soils after afforestation of agricultural lands,  
1272 EGU General Assembly 2024, Vienna, Austria, 14-19 April 2024, EGU24-9718,  
1273 <https://doi.org/10.5194/egusphere-egu24-9718>, 2024.

1274 Richardson, J., Chatterjee, A., & Darrel Jenerette, G.: Optimum temperatures for soil respiration  
1275 along a semi-arid elevation gradient in southern California, *Soil Biology and Biochemistry*, 46,  
1276 89-95, <https://doi.org/10.1016/j.soilbio.2011.11.008>, 2012.

1277 Riederer, M., Serafimovich, A., & Foken, T.: Net ecosystem CO<sub>2</sub> exchange measurements by the  
1278 closed chamber method and the eddy covariance technique and their dependence on atmospheric  
1279 conditions, *Atmos. Meas. Tech.*, 7(4), 1057-1064, <https://doi.org/10.5194/amt-7-1057-2014>,  
1280 2014.

1281 Roby, M. C., Scott, R. L., Biederman, J. A., Smith, W. K., & Moore, D. J. P.: Response of soil carbon  
1282 dioxide efflux to temporal repackaging of rainfall into fewer, larger events in a semiarid grassland,  
1283 *Frontiers in Environmental Science*, 10. <https://doi.org/10.3389/fenvs.2022.940943>, 2022.

1284 Rolo, V., Rivest, D., Maillard, É., & Moreno, G.: Agroforestry potential for adaptation to climate  
1285 change: A soil-based perspective, *Soil Use and Management*, 39(3), 1006-1032,  
1286 <https://doi.org/10.1111/sum.12932>, 2023.

1287 Rong, Y., Ma, L., Johnson, D., & Yuan, F.: Soil respiration patterns for four major land-use types of  
1288 the agro-pastoral region of northern China, *Agr. Ecosyst Environ.*, 213, 142-150,  
1289 <https://doi.org/10.1016/j.agee.2015.08.002>, 2015.

1290 Rosenstock, T. S., Mpanda, M., Pelster, D. E., Butterbach-Bahl, K., Rufino, M. C., Thiong'o, M., Mutuo,  
1291 P., Abwanda, S., Rioux, J., Kimaro, A. A., & Neufeldt, H.: Greenhouse gas fluxes from agricultural  
1292 soils of Kenya and Tanzania: GHG Fluxes From Agricultural Soils of East Africa, *Journal of*  
1293 *Geophysical Research: Biogeosciences*, 121(6), 1568-1580,  
1294 <https://doi.org/10.1002/2016JG003341>, 2016.

1295 Roupsard, O., Ferhi, A., Granier, A., Pallo, F., Depommier, D., Mallet, B., Joly, H. I., & Dreyer, E.:  
1296 Reverse Phenology and Dry-Season Water Uptake by *Faidherbia albida* (Del.) A. Chev. in an  
1297 Agroforestry Parkland of Sudanese West Africa, *Functional Ecology*, 13(4), 460-472,  
1298 <http://www.jstor.org/stable/2656552>, 1999.

1299 Roupsard, O., Audebert, A., Ndour, A. P., Clermont-Dauphin, C., Agbohessou, Y., Sanou, J., Koala, J.,  
1300 Faye, E., Sambakhe, D., Jourdan, C., le Maire, G., Tall, L., Sanogo, D., Seghier, J., Cournac, L., & Leroux,  
1301 L.: How far does the tree affect the crop in agroforestry? New spatial analysis methods in a  
1302 *Faidherbia* parkland, *Agr. Ecosyst. Environ.*, 296, 106928,  
1303 <https://doi.org/10.1016/j.agee.2020.106928>, 2020.

1304 Sarr, M.S., Diouf D., Roupsard O., Rocheteau A., Orange D., et al.: Estimation of seasonal water use  
1305 of *Faidherbia albida* (Delile) A.Chev. in a Sahelian agroforestry parkland, *Biotechnol. Agron. Soc.*  
1306 *Environ.*, 27(3), 196-204, <https://doi.org/10.25518/1780-4507.20512>, 2023.

1307 Schimel, J., Balsler, T. C., & Wallenstein, M.: Microbial stress-response physiology and its  
1308 implications for ecosystem function, *Ecology*, 88(6), 1386-1394, [https://doi.org/10.1890/06-](https://doi.org/10.1890/06-0219)  
1309 [0219](https://doi.org/10.1890/06-0219), 2007.

1310 Sida, T. S., Baudron, F., Kim, H., & Giller, K. E.: Climate-smart agroforestry: *Faidherbia albida* trees  
1311 buffer wheat against climatic extremes in the Central Rift Valley of Ethiopia, *Agr. Forest Meteorol.*,  
1312 248, 339-347, <https://doi.org/10.1016/j.agrformet.2017.10.013>, 2018.

1313 Siegwart, L., Bertrand, I., Roupsard, O., Duthoit, M., & Jourdan, C.: Root litter decomposition in a  
1314 sub-Saharan agroforestry parkland dominated by *Faidherbia albida*, *Journal of Arid*  
1315 *Environments*, 198, 104696, <https://doi.org/10.1016/j.jaridenv.2021.104696>, 2022.

1316 Siegwart, L., Bertrand, I., Roupsard, O., & Jourdan, C.: Contribution of tree and crop roots to soil  
1317 carbon stocks in a Sub-Saharan agroforestry parkland in Senegal, *Agr. Ecosyst. Environ.*, 352,  
1318 108524, <https://doi.org/10.1016/j.agee.2023.108524>, 2023.

1319 Sileshi, G. W.: The magnitude and spatial extent of influence of *Faidherbia albida* trees on soil  
1320 properties and primary productivity in drylands, *Journal of Arid Environments*, 132, 1-14,  
1321 <https://doi.org/10.1016/j.jaridenv.2016.03.002>, 2016.

1322 Sileshi, G. W., Teketay, D., Gebrekirstos, A., & Hadgu, K.: Sustainability of *Faidherbia albida*-Based  
1323 Agroforestry in Crop Production and Maintaining Soil Health., In J. C. Dagar, S. R. Gupta, & D.  
1324 Teketay (eds), *Agroforestry for Degraded Landscapes: Recent Advances and Emerging*  
1325 *Challenges—Vol. 2* (p. 349-369), Springer Singapore, [https://doi.org/10.1007/978-981-15-](https://doi.org/10.1007/978-981-15-6807-7_12)  
1326 [6807-7\\_12](https://doi.org/10.1007/978-981-15-6807-7_12), 2020.

1327 Singh, S., Mayes, M., Kivlin, S., & Jagadamma, S.: How the Birch Effect differs in mechanisms and  
1328 magnitudes due to soil texture, *Soil Biology and Biochemistry*, 179, 108973,  
1329 <https://doi.org/10.1016/j.soilbio.2023.108973>, 2023.

1330 Soudani, K., Hmimina, G., Delpierre, N., Pontailier, J. Y., Aubinet, M., Bonal, D., Caquet, B., de  
1331 Grandcourt, A., Burban, B., Flechard, C., Guyon, D., Granier, A., Gross, P., Heinesh, B., Longdoz, B.,  
1332 Loustau, D., Moureaux, C., Ourcival, J. M., Rambal, S., Saint André.L, Dufrene, E.: Ground-based  
1333 Network of NDVI measurements for tracking temporal dynamics of canopy structure and

1334 vegetation phenology in different biomes, *Remote Sensing of Environment*, 123, 234-245,  
1335 <https://doi.org/10.1016/j.rse.2012.03.012>, 2012.

1336 Skinner, R. H., & Wagner-Riddle, C.: Micrometeorological Methods for Assessing Greenhouse Gas  
1337 Flux., In M. A. Liebig, A. J. Franzluebbers, & R. F. Follett (eds) *Managing Agricultural Greenhouse*  
1338 *Gases: Coordinated Agricultural Research through GRACEnet to Address our Changing Climate* (p.  
1339 367-383), Elsevier, <https://doi.org/10.1016/B978-0-12-386897-8.00021-8>, 2012.

1340 Stephen, E. A., Evans, K. D., & Akwasi, A. A.: Effects of *Faidherbia albida* on some important soil  
1341 fertility indicators on agroforestry parklands in the semi-arid zone of Ghana, *Afr. J. Agr. Res.*,  
1342 15(2), 256-268, <https://doi.org/10.5897/ajar2019.14617>, 2020.

1343 Stetter, C., & Sauer, J.: Tackling climate change: Agroforestry adoption in the face of regional  
1344 weather extremes, *Ecological Economics*, 224, 108266,  
1345 <https://doi.org/10.1016/j.ecolecon.2024.108266>, 2024.

1346 Stojanović, M., Jocher, G., Kowalska, N., Szatniewska, J., Zavadilová, I., Urban, O., Čáslavský, J.,  
1347 Horáček, P., Acosta, M., Pavelka, M., & Marshall, J. D.: Disaggregation of canopy photosynthesis  
1348 among tree species in a mixed broadleaf forest, *Tree Physiology*, 44(7), tpae064,  
1349 <https://doi.org/10.1093/treephys/tpae064>, 2024.

1350 Tagesson, T., Ardö, J., Guiro, I., Cropley, F., Mbow, C., Horion, S., Ehammer, A., Mougín, E., Delon, C.,  
1351 Galy-Lacaux, C., & Fensholt, R.: Very high CO<sub>2</sub> exchange fluxes at the peak of the rainy season in a  
1352 West African grazed semi-arid savanna ecosystem, *Geografisk Tidsskrift - Danish Journal of*  
1353 *Geography*, 116(a), 93-109, <https://doi.org/10.1080/00167223.2016.1178072>, 2016.

1354 Tagesson, T., Fensholt, R., Cappelaere, B., Mougín, E., Horion, S., Kergoat, L., Nieto, H., Mbow, C.,  
1355 Ehammer, A., Demarty, J., & Ardö, J.: Spatiotemporal variability in carbon exchange fluxes across  
1356 the Sahel, *Agr. Forest Meteorol.*, 226-227(b), 108-118,  
1357 <https://doi.org/10.1016/j.agrformet.2016.05.013>, 2016.

1358 Tagesson, T., Fensholt, R., Cropley, F., Guiro, I., Horion, S., Ehammer, A., & Ardö, J.: Dynamics in  
1359 carbon exchange fluxes for a grazed semi-arid savanna ecosystem in West Africa. *Agr. Ecosyst.*  
1360 *Environ.*, 205, 15-24, <https://doi.org/10.1016/j.agee.2015.02.017>, 2015.

1361 Tang, J., Bolstad, P. V., Desai, A. R., Martin, J. G., Cook, B. D., Davis, K. J., & Carey, E. V.: Ecosystem  
1362 respiration and its components in an old-growth forest in the Great Lakes region of the United  
1363 States, *Agr. Forest Meteorol.*, 148(2), 171-185, <https://doi.org/10.1016/j.agrformet.2007.08.008>,  
1364 2008.

- 1365 Tang, X., Carvalhais, N., Moura, C., Ahrens, B., Koirala, S., Fan, S., Guan, F., Zhang, W., Gao, S.,  
1366 Magliulo, V., Buysse, P., Liu, S., Chen, G., Yang, W., Yu, Z., Liang, J., Shi, L., Pu, S., & Reichstein, M.:  
1367 Global variability of carbon use efficiency in terrestrial ecosystems, *Biogeochemistry: Land*,  
1368 <https://doi.org/10.5194/bg-2019-37>, 2019.
- 1369 Tucker, C. L., & Reed, S. C.: Low soil moisture during hot periods drives apparent negative  
1370 temperature sensitivity of soil respiration in a dryland ecosystem: A multi-model comparison,  
1371 *Biogeochemistry*, 128(1-2), 155-169, <https://doi.org/10.1007/s10533-016-0200-1>, 2016.
- 1372 Unger, S., Máguas, C., Pereira, J. S., David, T. S., & Werner, C.: The influence of precipitation pulses  
1373 on soil respiration – Assessing the “Birch effect” by stable carbon isotopes, *Soil Biology and*  
1374 *Biochemistry*, 42(10), 1800-1810, <https://doi.org/10.1016/j.soilbio.2010.06.019>, 2010.
- 1375 Valujeva, K., Pilecka-Ulcugaceva, J., Skiste, O., Liepa, S., Lagzdins, A., & Grinfelde, I.: Soil tillage and  
1376 agricultural crops affect greenhouse gas emissions from Cambic Calcisol in a temperate climate,  
1377 *Acta. Agr. Scand. B-S-P.*, 72(1), 835-846, <https://doi.org/10.1080/09064710.2022.2097123>,  
1378 2022.
- 1379 Van Haren, J. L. M., De Oliveira, R. C., Restrepo-Coupe, N., Hutyra, L., De Camargo, P. B., Keller, M.,  
1380 & Saleska, S. R.: Do plant species influence soil CO<sub>2</sub> and N<sub>2</sub>O fluxes in a diverse tropical forest?  
1381 *Journal of Geophysical Research: Biogeosciences*, 115, G03010,  
1382 <https://doi.org/10.1029/2009JG001231>, 2010.
- 1383 Vargas, R., Enrique, S. C. P., Serrano-Ortiz, P., Yuste, J. C., Domingo, F., López-Ballesteros, A., &  
1384 Oyonarte, C.: Hot-moments of soil CO<sub>2</sub> efflux in a water-limited grassland, *Soil Systems*, 2(3), 1-18,  
1385 <https://doi.org/10.3390/soilsystems2030047>, 2018.
- 1386 Vickers, D., & Mahrt, L.: Quality Control and Flux Sampling Problems for Tower and Aircraft Data,  
1387 *Journal of Atmospheric and Oceanic Technology*, 14(3), 512-526,  
1388 [http://dx.doi.org/10.1175/1520-0426\(1997\)014%3C0512:QCAFSP%3E2.0.CO;2](http://dx.doi.org/10.1175/1520-0426(1997)014%3C0512:QCAFSP%3E2.0.CO;2), 1997.
- 1389 Wachiye, S., Merbold, L., Vesala, T., Rinne, J., Räsänen, M., Leitner, S., & Pellikka, P.: Soil greenhouse  
1390 gas emissions under different land-use types in savanna ecosystems of Kenya, *Biogeosciences*,  
1391 17(8), 2149-2167, <https://doi.org/10.5194/bg-17-2149-2020>, 2020.
- 1392 Wang, M., Guan, D.-X., Han, S.-J., & Wu, J.-L.: Comparison of eddy covariance and chamber-based  
1393 methods for measuring CO<sub>2</sub> flux in a temperate mixed forest, *Tree Physiology*, 30(1), 149-163,  
1394 <https://doi.org/10.1093/treephys/tpp098>, 2010.

1395 Wang, Z., Ji, L., Hou, X., & Schellenberg, M. P.: Soil Respiration in Semiarid Temperate Grasslands  
1396 under Various Land Management, PLOS ONE, 11(1), e0147987,  
1397 <https://doi.org/10.1371/journal.pone.0147987>, 2016.

1398 Waring E., Quinn M., McNamara A., Arino de la Rubia E., Zhu H., Ellis S.: skimr: Compact and  
1399 Flexible Summaries of Data, R package (version 2.1.5), <https://github.com/ropensci/skimr/>,  
1400 <https://docs.ropensci.org/skimr/> (website), 2024.

1401 Warren, C. R. Response of osmolytes in soil to drying and rewetting. Soil Biology and Biochemistry,  
1402 70, 22-32, <https://doi.org/10.1016/j.soilbio.2013.12.008>, 2014.

1403 Webb, E. K., Pearman, G. I., & Leuning, R., Correction of flux measurements for density effects due  
1404 to heat and water vapour transfer. Q. J. R. Meteorol. Soc., 106, 85-100,  
1405 <https://doi.org/10.1002/qj.49710644707>, 1980.

1406 Wieckowski, A., Vestin, P., Ardó, J., Roupsard, O., Ndiaye, O., Diatta, O., Ba, S., Agbohessou, Y.,  
1407 Fensholt, R., Verbruggen, W., Gebremedhn, H. H., & Tagesson, T.: Eddy covariance measurements  
1408 reveal a decreased carbon sequestration strength 2010–2022 in an African semiarid savanna,  
1409 Glob. Change Biol., 30(9), e17509. <https://doi.org/10.1111/gcb.17509>, 2024.

1410 Wiesner, S., Desai, A. R., Duff, A. J., Metzger, S., & Stoy, P. C.: Quantifying the natural climate solution  
1411 potential of agricultural systems by combining eddy covariance and remote sensing. Journal of  
1412 Geophysical Research: Biogeosciences, 127(9), e2022JG006895,  
1413 <https://doi.org/10.1029/2022JG006895>, 2022.

1414 Wild, J., Kopecký, M., Macek, M., Šanda, M., Jankovec, J., & Haase, T.: Climate at ecologically relevant  
1415 scales: A new temperature and soil moisture logger for long-term microclimate measurement,  
1416 Agr. Forest Meteorol., 268, 40-47, <https://doi.org/10.1016/j.agrformet.2018.12.018>, 2019.

1417 Williams, C.A., Hanan, N.P., Neff, J.C. et al.: Africa and the global carbon cycle, Carbon Balance  
1418 Manage, 2, 3, <https://doi.org/10.1186/1750-0680-2-3>, 2007.

1419 Williams, C. A., Hanan, N., Scholes, R. J., & Kutsch, W.: Complexity in water and carbon dioxide  
1420 fluxes following rain pulses in an African savanna, Oecologia, 161(3), 469-480,  
1421 <https://doi.org/10.1007/s00442-009-1405-y>, 2009.

1422 Wohlfahrt, G., & Galvagno, M.: Revisiting the choice of the driving temperature for eddy covariance  
1423 CO<sub>2</sub> flux partitioning, Agr. Forest Meteorol., 237-238, 135-142,  
1424 <https://doi.org/10.1016/j.agrformet.2017.02.012>, 2017.

1425 Wutzler, T., Lucas-Moffat, A., Migliavacca, M., Knauer, J., Sickel, K., Šigut, L., Menzer, O., and  
1426 Reichstein, M.: Basic and extensible post-processing of eddy covariance flux data with REddyProc,  
1427 Biogeosciences, 15, 5015–5030, <https://doi.org/10.5194/bg-15-5015-2018>, 2018.

1428 Xenakis, G.: FREddyPro: Post-Processing EddyPro Full Output File. Edinburgh, UK. R package  
1429 version 1.0.1., 2016.

1430 Xue, H., & Tang, H.: Responses of soil respiration to soil management changes in an agropastoral  
1431 ecotone in Inner Mongolia, China, Ecology and Evolution, 8(1), 220-230,  
1432 <https://doi.org/10.1002/ece3.3659>, 2018.

1433 Yan, L., Chen, S., Xia, J., & Luo, Y.: Precipitation regime shift enhanced the rain pulse effect on soil  
1434 respiration in a semi-arid steppe, PLoS ONE, 9(8),  
1435 <https://doi.org/10.1371/journal.pone.0104217>, 2014.

1436 Yu, H., Xu, Z., Zhou, G., & Shi, Y.: Soil carbon release responses to long-term versus short-term  
1437 climatic warming in an arid ecosystem, Biogeosciences, 17(3), 781-792,  
1438 <https://doi.org/10.5194/bg-17-781-2020>, 2020.

1439 Yu, T., Jiapaer, G., Bao, A., Zheng, G., Zhang, J., Li, X., Yuan, Y., Huang, X., & Umhuza, J.: Disentangling  
1440 the relative effects of soil moisture and vapor pressure deficit on photosynthesis in dryland  
1441 Central Asia, Ecological Indicators, 137, 108698, <https://doi.org/10.1016/j.ecolind.2022.108698>,  
1442 2022.

1443 Yu, X., Zha, T., Pang, Z., Wu, B., Wang, X., Chen, G., Li, C., Cao, J., Jia, G., Li, X., & Wu, H.: Response of  
1444 soil respiration to soil temperature and moisture in a 50-year-old oriental arborvitae plantation  
1445 in China, PLoS ONE, 6(12), <https://doi.org/10.1371/journal.pone.0028397>, 2011.

1446 Zaman M., Kleinedam K., Bakken L., Berendt J., Bracken C., Butterbach-Bahl K., Cai Z., Chang S. X.,  
1447 Clough T., Dawar K., Ding W. X., Dörsch P., dos Reis Martins M., Eckhardt C., Fiedler S., Frosch T.,  
1448 Goopy J., Görres C.-M., Gupta A., Henjes S., Hofmann M. E. G., Horn M. A., Jahangir M. M. R., Jansen-  
1449 Willems A., Lenhart K., Heng L., Lewicka-Szczebak D., Lucic G., Merbold L., Mohn J., Molstad L.,  
1450 Moser G., Murphy P., Sanz-Cobena A., Šimek M., Urquiaga S., Well R., Wrage-Mönnig N., Zaman S.,  
1451 Zhang J., Müller C.: Greenhouse Gases from Agriculture. In M. Zaman, L. Hang, C. Müller (eds)  
1452 Measuring emission of agricultural greenhouse gases and developing mitigation options using  
1453 nuclear and related techniques Springer, Cham, [https://doi.org/10.1007/978-3-030-55396-8\\_1](https://doi.org/10.1007/978-3-030-55396-8_1),  
1454 2021.

1455 Zeileis, A., Grothendieck, G., Ryan, J. A., Ulrich, J. M., & Andrews, F.: Package 'zoo': S3 Infrastructure  
1456 for Regular and Irregular Time Series (Z's Ordered Observations) (version 1.8-12) [R Package],  
1457 <https://zoo.R-Forge.R-project.org/>, 2024.

1458 Zhang, X., Bi, J., Zhu, D., & Meng, Z.: Seasonal variation of net ecosystem carbon exchange and gross  
1459 primary production over a Loess Plateau semi-arid grassland of northwest China, *Scientific*  
1460 *Reports*, 14(1), 2916, <https://doi.org/10.1038/s41598-024-52559-6>, 2024.

1461 Zhang, X., Ramakanth, K. K., & Long, Y.: The biomechanics of turgor pressure, *Current Biology*,  
1462 34(20), R986-R991, <https://doi.org/10.1016/j.cub.2024.07.013>, 2024.

1463 Zhao, C., Miao, Y., Yu, C., Zhu, L., Wang, F., Jiang, L., Hui, D., & Wan, S.: Soil microbial community  
1464 composition and respiration along an experimental precipitation gradient in a semiarid steppe,  
1465 *Scientific Reports*, 6(1), 24317, <https://doi.org/10.1038/srep24317>, 2016.

1466 Zhou, Y., Williams, C. A., Lauvaux, T., Feng, S., Baker, I. T., Wei, Y., Denning, A. S., Keller, K., & Davis,  
1467 K. J.: ACT-America: Gridded Ensembles of Surface Biogenic Carbon Fluxes, 2003-2019 (Version  
1468 1.1), ORNL Distributed Active Archive Center, <https://doi.org/10.3334/ORNLDAAC/1675>, 2019.

1469 Zhou, Y., Williams, C. A., Lauvaux, T., Davis, K. J., Feng, S., Baker, I., et al.: A multiyear gridded data  
1470 ensemble of surface biogenic carbon fluxes for North America: Evaluation and analysis of results,  
1471 *Journal of Geophysical Research: Biogeosciences*, 125, e2019JG005314,  
1472 <https://doi.org/10.1029/2019JG005314>, 2020.